

Neural networks versus Logistic regression for 30 days all-cause readmission prediction

Ahmed Allam^{*1,2}, Mate Nagy^{†3}, George Thoma^{‡5}, and Michael Krauthammer^{§1,2,3,4}

¹Department of Quantitative Biomedicine, University of Zurich

²Biomedical Informatics Group, University Hospital of Zurich

³Program in Computational Biology and Bioinformatics, Yale University

⁴Department of Pathology, Yale School of Medicine

⁵Lister Hill National Center for Biomedical Communications, National Library of Medicine

Abstract

Heart failure (HF) is one of the leading causes of hospital admissions in the US. Readmission within 30 days after a HF hospitalization is both a recognized indicator for disease progression and a source of considerable financial burden to the healthcare system. Consequently, the identification of patients at risk for readmission is a key step in improving disease management and patient outcome. In this work, we used a large administrative claims dataset to (1) explore the systematic application of neural network-based models versus logistic regression for predicting 30 days all-cause readmission after discharge from a HF admission, and (2) to examine the additive value of patients' hospitalization timelines on prediction performance. Based on data from 272,778 (49% female) patients with a mean (SD) age of 73 years (14) and 343,328 HF admissions (67% of total admissions), we trained and tested our predictive readmission models following a stratified 5-fold cross-validation scheme. Among the deep learning approaches, a recurrent neural network (RNN) combined with conditional random fields (CRF) model (RNNCRF) achieved the best performance in readmission prediction with 0.642 AUC (95% CI, 0.640-0.645). Other models, such as those based on RNN, convolutional neural networks and CRF alone had lower performance, with a non-timeline based model (MLP) performing worst. A competitive model based on logistic regression with LASSO achieved a performance of 0.643 AUC (95% CI, 0.640-0.646). We conclude that data from patient timelines improve 30 day readmission prediction for neural network-based models, that a logistic regression with LASSO has equal performance to the best neural network model and that the use of administrative data result in competitive performance compared to published approaches based on richer clinical datasets.

*ahmed.allam@uzh.ch

†mate.nagy@yale.edu

‡gthoma@mail.nih.gov

§michael.krauthammer@uzh.ch

1 Introduction

Heart failure (HF) is one of the leading causes for hospital admissions in the US [1–4] with high numbers of readmissions within 30 days of discharge [2–4]. Based on multiple hospitalization data sources, the yearly rate of 30 days all-cause readmission after an HF hospitalization is approximately 23-24% [1, 2, 5], posing a huge burden on the healthcare system with an estimated cost of \$17 billions of total Medicare expenditure [4, 6]. Beyond the associated expenses and costs, readmissions have negative consequences on patients’ health status, leading to complications and increased risk of disease progression [6]. Efforts toward quality improvement such as introducing programs that incentivize and penalize hospitals based on the yearly readmission rate have been the focus of researchers and policy makers [2, 7]. Likewise, there has been increasing interest in developing predictive models and/or monitoring systems that allow for prevention and preemptive steps, such as the prediction of 30 days all-cause readmission for patients hospitalized with HF for which many challenges remain [8, 9].

In this paper, we aim at exploring the systematic application of neural network models for predicting 30 days all-cause readmission after discharge from a HF hospitalization (which we call index event below). Concretely, given a set of sequences of hospitalization admissions with their corresponding 30 days all-cause readmission outcome, we seek to predict the 30 days all-cause readmission of the last HF admission (i.e. the last index event) in each sequence. The sequence of hospitalization events for each patient will be referred to as “*timeline*” and “*trajectory*” interchangeably throughout the paper. Published approaches chiefly use data from the index event for predicting hospital readmission, paying less attention to a patient’s trajectory leading to the current heart failure admission. Intuitively, a patient’s history may add much additional information that may be informative of whether a patient is subject to early readmission. For example, a history of multiple readmissions in the past may be a risk factor for future readmissions. Consequently, one specific aim of this study is to examine the value of including a patient’s trajectory data in a 30 day readmission prediction model. To this end, we examine three approaches for modeling the problem of which two use the temporal information encoded in the patients’ trajectories (sequence labeling and sequence classification), and one that does not (index event classification). Particularly, we implemented multiple neural network models with varying architectures and objective functions such as recurrent neural networks (RNN), and convolutional neural networks (CNN) as examples of sequence labeling and classification approaches, and multilayer perceptron (MLP) along with logistic regression as baseline models representing the index event classification approach. We conducted these studies with a large administrative claims dataset, which lacks the detailed clinical information found in datasets typically used for this problem. As claims data are readily available and can be robustly harmonized, they pose less privacy concerns and are ideally suited for tackling the HF readmission problem.

2 Methods

2.1 Dataset

The HF dataset was derived from the Healthcare Cost and Utilization Project (HCUP), Nationwide Readmission Database (NRD), issued by the Agency for Healthcare Research and Quality (AHRQ) [10]. It includes patients’ discharges (i.e. hospital claims) of all-payer hospital inpatient stays over the 2013 period that are contributed by twenty one states and accounting for 49.1% of all US hospitalizations [10]. Each claim in the dataset is associated with a corresponding patient who is identified by a uniquely generated linkage number (“*visitlink*”) that tracks the patient’s visits across hospitals within a state. Each claim represents a summary of an inpatients hospitalization event, including information about the hospitalization event such as the time of admission and discharge, the diagnosis, procedures, comorbidity and chronic conditions, length of stay, along other clinical fields associated with the event (a detailed description of the data elements can be found at [11]). Moreover, as each claim is linked to a patient identifier, it also includes patient’s socio-demographic information such as age, gender, income category and place location based on the National Center for Health Statistics (NCHS) classification scheme for US counties.

2.1.1 Timeline/trajectory building and processing

We built timelines/sequences out of the claims, allowing us to preserve the temporal progression and the history of hospitalization events for every patient. Patients were included in the HF dataset if they met the following conditions:

1. had at least one hospitalization event between January and November period with HF as the primary diagnosis (i.e. congestive heart failure; code = 108) as determined by Clinical Classification Software (CCS) that groups International Classification of Diseases, Version 9 (ICD-9) codes [12]
2. were ≥ 18 years old when they had an HF hospitalization event

Formally, we denote each claim (i.e. hospitalization event) by a feature vector \bar{x}_t describing the characteristics and attributes of the hospitalization event and the corresponding patient. Moreover, we denote its corresponding label by $y_t \in \{0, 1\}$, representing the 30 days all-cause readmission. The readmission outcome was computed based on the AHRQ HCUP 30-day readmission measure (see Appendix A in [15]).

To determine if $y_t = 1$ (i.e. the hospital admission of the future claim/event \bar{x}_{t+1} occurs within 30 days from the current event \bar{x}_t), we traverse the patient’s timeline (temporally-ordered hospitalization events) from left to right and check if:

1. the current event \bar{x}_t is an index event (i.e. an event where HF is the primary diagnosis as indicated by CCS diagnosis grouper; code = 108) and
2. the difference between the admission of the next event \bar{x}_{t+1} and the discharge of current event \bar{x}_t is ≤ 30 days (i.e. $\Delta t \leq 30$ days)

Figure 1: An example of a patient’s timeline with 30 days all-cause readmission labeling

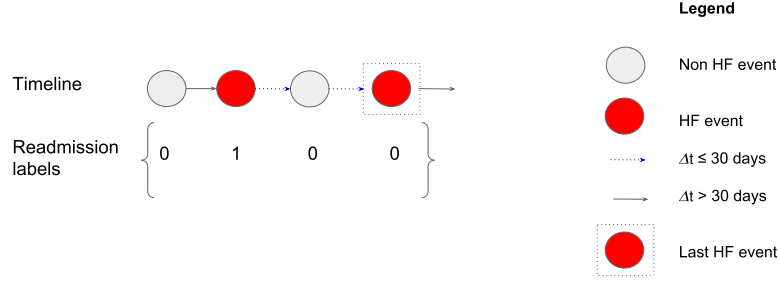


Figure 1 depicts the labeling process of a patient’s timeline. Notice the final event will always be the last HF event in a patient’s timeline for which we can determine its readmission label.

2.1.2 Dataset features

Each claim/event in a patient’s timeline was represented by a feature vector \bar{x}_t encoding the characteristics of the hospitalization event and the corresponding patient. The feature vector included most of the fields included in the NRD databases describing every inpatients hospitalization event such as the time of admission and discharge, the diagnosis, procedures, comorbidity and chronic conditions, length of stay, along other clinical fields associated with the event. A detailed description of all the used features is found in the supplementary material.

2.2 Models and notation

2.2.1 Sequence labeling and classification

In this section, we introduce the sequence labeling approach to 30 days all-cause readmission prediction. Generally, given a patient’s temporally ordered sequence of claims $\underline{\mathbf{x}} = [\bar{x}_1, \dots, \bar{x}_t, \dots, \bar{x}_T]$, represented by a d -dimensional feature vector $\bar{x}_t \in \mathbb{R}^d$, we seek a labeling $\underline{\mathbf{y}} = [y_1, \dots, y_t, \dots, y_T]$ representing the 30 days all-cause readmission outcomes where $y_t \in \{0, 1\}$ and T is the patient-specific sequence length (i.e. equivalent to T_i where i refers to the i -th patient in training dataset). Given a training set $D_{train} = \{(\mathbf{x}_i, \mathbf{y}_i)\}_{i=1}^N$, the goal is to learn a model (i.e. function map f) by minimizing an objective function $L(f, D_{train})$ that measures the discrepancy between every sequence’s target labels $\underline{\mathbf{y}}_i$ and its corresponding predicted label sequence $\hat{\underline{\mathbf{y}}}_i$ in the training dataset. A common

approach is to use a parametrized function $f(\boldsymbol{\theta})$ such that learning the best function map (i.e. training a model) translates into finding the optimal weights $\boldsymbol{\theta}$ where $\boldsymbol{\theta} = \arg \min_{\boldsymbol{\theta}} L(f, D_{train})$. With the choice of a differentiable function, the optimal weights $\boldsymbol{\theta}$ are obtained through an iterative process by using the gradient of the objective function $\nabla_{\boldsymbol{\theta}} L(f, D_{train})$, scaling it with step size η , and subtracting the result from the current weights at each iteration. Intuitively, the weights update equation

$$\boldsymbol{\theta}^{k+1} = \boldsymbol{\theta}^k - \eta \nabla_{\boldsymbol{\theta}^k} L(f, D_{train}) \quad (1)$$

is directing the new weights toward the steepest descent (i.e. the direction which minimizes $L(f, D_{train})$) at each update iteration k . Sequence classification is similar to sequence labeling but instead of assigning labels/classes to each event in the sequence, one assigns one single label/class to the whole sequence. Thus, in the sequence labeling setting, the trained model will predict an outcome for every event in the sequence, while in the sequence classification setting, the model predicts the class of the whole sequence. In this work, the difference between both approaches is mainly in the training phase (learning the labels of all events versus one single label for the sequence), while during the testing phase, both models are used to predict the outcome/label of the last HF event. The latter is directly provided through sequence labeling. In sequence classification, we are using the label of the last HF event as a substitute for the sequence label and a training loss that is associated with that event. To summarize, we use the term “labeling” and “classification” to differentiate between models incorporating the labels of previous events in the training/learning of the model versus optimizing only on the last HF event label. In all cases, the testing/decoding phase is equivalent and is focused on the prediction of the label/class of the last HF event.

2.2.2 Recurrent neural network (RNN)

Recurrent neural networks (RNN) is a connectionist model that is well suited for modeling sequential and temporal data with varying length [16–18]. A basic RNN is similar to feed-forward neural network but with additional support for cyclical connections (i.e. recurrent edges among the hidden layers at different time steps) [17, 18]. RNNs computes a hidden vector at each time step (i.e. state vector \bar{h}_t at time t), representing a history or context summary of the sequence using the input and hidden states vector from the previous time step. This allows the model to learn long-range dependencies where the network is unfolded as many times as the length of the sequence it is modeling. To compute the outcome \hat{y}_t at time t , an affine transformation followed by non-linear activation function σ is applied to the state vector \bar{h}_t . The non-linear operator σ can be either the *sigmoid* function applied to a scalar input or its generalization to multi-class *softmax* function applied to vector. As a result, the outcome \hat{y}_t represents a probability distribution over the set of possible labels at time t . Gradient descent (i.e. “*vanilla*” gradient descent as in Equation 1 or any variant) is used for optimizing the weights of the network while the gradient is computed using back propagation through time [19]. Although RNNs are capable of handling and representing variable-length sequences, in practice, the learning process faces challenges due to the vanishing/exploding gradient problem [17, 20, 21]. To overcome these challenges, gradient clipping [22] and

gated memory cells approach as in long short-term memory (LSTM) and gated recurrent unit (GRU) [23–25] were proposed replacing the conventional nodes in the hidden layer and hence updating the computation mechanism of the hidden state vector \bar{h}_t .

2.2.3 RNN objective function

We defined the loss at each time step for an i -th sequence by the cross-entropy error/loss

$$l_t^{(i)} = - \sum_{c=1}^{|V_{label}|} y_{t,c}^{(i)} \times \log(\hat{y}_{t,c}^{(i)}) \quad (2)$$

where V_{label} is set of admissible classes, $|V_{label}|$ is the number of classes, $y_{t,c} \in \{0, 1\}$ is equivalent to $\mathbb{1}[y_t = c]$ (i.e. a boolean indicator that is equal to 1 when c is the reference/ground-truth class at time t), and $\hat{y}_{t,c}$ is the probability of the class c at time t . Four realizations/definitions of objective functions were tested in this study. Given that our focus is on the 30 days all-cause readmissions for the last HF hospitalization event, the first loss (Convex_HF_lastHF) was defined by a convex combination between the average loss from all HF events in patient’s timeline and the loss from the last HF event. The convex combination is parametrized by parameter α that was determined using a validation set inspired by the work done in [26]. The second loss function (LastHF) used the loss computed only from the last HF event while the third (Uniform_HF) uniformly averaged the loss from all HF events in a patient’s timeline. Lastly, the fourth objective function (Convex_HF_NonHF) was based on a convex combination between the average loss contributed by all HF events in patient’s timeline and the average loss from the non HF events.

The objective function for the whole training set D_{train} was defined by the average loss L_i across all the sequences in D_{train} plus a weight regularization term (i.e. l_2 -norm regularization) applied to the model parameters represented by θ

$$L_i = \frac{1}{T_i} \sum_{t=1}^{T_i} l_t^{(i)} \quad (3)$$

$$L(\theta) = \frac{1}{N} \sum_{i=1}^N L_i + \frac{\lambda}{2} \|\theta\|_2^2 \quad (4)$$

In addition to the l_2 -norm regularization in the objective function, we also experimented with dropout [27] by deactivating neurons in the network layers using probability $p_{dropout}$ in order to reduce the network’s chances of overfitting the training set .

2.2.4 RNN with scheduled sampling (RNNSS)

Another variation of the RNN model that we experimented with is using a scheduled sampling approach (“teacher forcing”) [28] while training the RNN model. Again we used the same four definitions of the loss functions used in the RNN case.

2.2.5 Conditional random fields (CRF)

Although RNN models are suited for modeling temporal data, the outcome/label prediction for each event is performed independently from each other. That is: the labeling decision is done *locally* (i.e. without considering any association/correlation between neighboring labels). In other words, there is a need for a joint modeling approach that is *global* by considering the whole sequence of labels when performing the optimization and inference. Linear-chain CRF suits this requirement well by modeling the probability of the whole labeled sequence (i.e. outcome sequence) given the input sequence. It is a class of undirected discriminative graphical models that uses a global feature function within a log-linear model formalism, making it well suited for structured prediction [29]. In this study, we applied CRF in two occasions with two variations (i.e. definition of potential functions).

2.2.6 CRF with RNN

We first experimented with combining the RNN model with a CRF layer by feeding the computed features from the RNN layer as inputs to the CRF layer as in [30]. We denote the output features of the RNN layer by $\underline{\mathbf{z}} = [\bar{z}_1, \bar{z}_2, \dots, \bar{z}_T]$ representing the sequence of output features computed from the input sequence $\underline{\mathbf{x}}$ (both sequences have equal length). The potential functions in the CRF layer were computed using $\underline{\mathbf{z}}$ along with label sequence $\underline{\mathbf{y}}$ in two variations:

1. RNNCRF (Unary) that computed unary potential by using only the RNN output feature vector to generate an output vector with dimension equal to the number of classes $|V_{label}|$ for each \bar{z}_t . The pairwise potential is modeled using a transition parameters matrix $A(y_{t-1}, y_t)$ of size $|V_{label}| \times |V_{label}|$ representing the transition score from one outcome class to another.
2. RNNCRF (Pairwise) that computes pairwise potentials using both the RNN output feature vectors and the labels sequence such that it generates an output vector of size $|V_{label}| \times |V_{label}|$ at every time step t similar to the approach reported in [31].

2.2.7 CRF & Neural CRF

We also tested a CRF approach without the RNN block. The first used CRF only (i.e. first-order linear chain CRF) model using the two variations of potential functions (i.e. unary and pairwise). The second model is combining CRF with neural model (i.e. using non-linear transformation for computing features) similar to the approach in [32] using the same two potential function variants. The objective function for models that incorporated CRF was defined by the negative conditional log-likelihood $L(\theta)$ plus an l_2 -norm weight regularization term,

$$L(\theta) = \left[\frac{1}{N} \sum_{i=1}^N -\log(p(\underline{\mathbf{y}}_i | \underline{\mathbf{x}}_i)) \right] + \frac{\lambda}{2} \|\theta\|_2^2 \quad (5)$$

Estimating the optimal weights θ is typically done by applying a variant of gradient descent algorithm (as described in Equation 1) where the sum-product algorithm (i.e. performing a variation of the forward-backward algorithm [33])

is used. Decoding the sequence (i.e. finding the optimal labeling $\hat{\underline{y}}_{optimal}$) is done through a variant of Viterbi algorithm [34, 35].

2.2.8 Convolutional neural networks (CNN)

The CNN models adopt the sequence classification view by using the $2D$ arrangement of the patients’ timelines with an objective function defined only for the last HF event (i.e. the loss function is defined for the last HF event that we seek to predict its readmission outcome). A CNN model is a feed-forward neural network that typically consists of multiple layers of which *convolutional* layer is the building block. A convolutional layer is composed of filters/kernels (in our context, the kernel is a $2D$ arrangement of weights in matrix form) that are convolved with the features of the previous layer (such as the input layer) to produce feature maps. More formally, a patient’s timeline was arranged in a matrix form where the sequence of events are stacked (i.e. concatenated) to form a matrix $X = [\bar{x}_1 \ \bar{x}_2 \ \dots \ \bar{x}_{T_{max}}]^T$ of size $T_{max} \times d$ where d is the dimension of an event vector \bar{x}_t and T_{max} is the maximum length of a patient’s timeline in the training set – patients with shorter timelines are padded to have a common representation. A kernel F is a matrix of weights that is convolved with X to produce a feature map M such that an entry in M is computed by first taking the sum of element-wise multiplication of the weights in the kernel F and the corresponding input of the previous layer, then adding a bias term followed by non-linear operation. Typically, multiple kernels are applied and the resulting feature maps are stacked on top of each other forming a $3D$ volume/tensor to be processed subsequently in the next layers. The elements of each kernel represent the shared parameters that we optimize during the training phase. Another type of layers in this network is a *pooling* layer that also includes kernels/filters but with no trainable weights, which slides over the input feature maps based on a defined horizontal and vertical stride size and computes a summary score such as a maximum or average score for every region of overlap. As a result, in the pooling layer we can change the size of the generated feature maps by specifying the stride and padding size such that the size of the feature maps decreases as we progress into subsequent layers in the network (i.e. equivalent to subsampling). Another commonly used layer after the convolutional/pooling layers is the *fully-connected* layer (FC). FC takes an input vector from the reshaped feature maps generated in the last convolutional/pooling layers and applies an affine transformation followed by non-linear element-wise operation. In this work, we experimented with two types of convolutional models:

1. CNN model that describes a network inspired by commonly used models in computer vision and image processing research [40] that makes use of multiple small square convolutional and pooling kernels, where the generated feature maps are reduced in size as a function of the network depth (i.e. number of layers) until reaching to the fully-connected layer/s.
2. CNN-Wide model that adapts the approach used by Kim [41] for sentence classification where the convolutional kernels are wide/rectangular covering the whole input feature dimension. In other words, a kernel in this model would have varying sizes (such as $2 \times d$, $3 \times d$, $5 \times d$) where the convolution is applied to the whole feature vector for two or more events for every possible window of events in the patient’s timeline (i.e. applied

to matrix X). After each convolution operation, the result is a vector of feature map for every kernel. In this network, the pooling layer reduces each generated feature map vector to a scalar (i.e. one feature) and then concatenates each one of them into one vector having number of elements equal to the number of applied convolutional kernels. Lastly, the resulting vector is passed into one or more FC layers before it is passed to the output layer.

Both CNN models use an output layer where the computed vector of activations/feature map in the penultimate layer are passed to generate a probability distribution over the outcome labels (as in the RNN case). The defined loss function for every sequence in both models is the loss computed for the last HF event as in the RNN case (see LastHF in Section 2.2.3) where the overall objective function for the training set is also equivalent to RNN case (Equation 4).

2.2.9 Multilayer perceptron (MLP)

A final neural network-based model is the multilayer perceptrons which is also a feed-forward neural network (MLP). The MLP network is composed of an input layer then a set of multiple FC layers and lastly an output layer that generates a probability distribution over the outcome classes. The FC layers, as we discussed earlier, mainly consists of two operations; an affine transformation followed by non-linear element-wise operation to generate new feature vectors (i.e. learned representations). The difference between this modeling approach and the previous ones is that MLP takes the *event* view of the problem by modeling the last index event \bar{x}_T only and discarding the sequence aspect of the patients' timeline. The defined loss and the overall objective function is equivalent to the ones defined for the RNN case (LastHF) and Equation 4.

2.2.10 Logistic regression (LR)

Logistic regression (LR) is a commonly used model for classification problems due to its simplicity and model interpretability. Like MLP, LR supports the *event* view of the problem by modeling only the last index event. LR model can be considered as a neural network model with no hidden layers and one output neuron. In this setup, the input features are fully-connected to one output neuron where the *sigmoid* function is applied as a non-linear operation computing the probability of the outcome label to be equal to 1. In other words, the LR model computes $p(\hat{y}_T = 1|\bar{x}_T) = \frac{1}{1+\exp^{-(\mathbf{w}_{1 \times d}\bar{\mathbf{x}}_T+\mathbf{b})}}$ where $\mathbf{W}_{1 \times d}$ is the weight matrix that maps \bar{x}_T to a scalar value (i.e. using one neuron), b is the bias term and $\frac{1}{1+\exp^{-z}}$ is the *sigmoid* function representing the non-linear operation. The output represents the probability of a patient readmitting to hospital within 30 days after HF hospitalization event. In this work, LR was the baseline model that we compare its performance to the ones of the neural network-based models. The loss function for each patient's last event is defined by the conditional log-likelihood which is equivalent to the cross-entropy loss for the binary case (i.e 2-class classification) and the overall objective function is based on the average conditional log-likelihood of the data (see Equation 4). Additionally, we experimented with two regularization schemes: (1) l_1 -norm regularization (LASSO) and (2) l_2 -norm regularization.

3 Experimental setup

We followed a stratified 5-fold cross-validation scheme, in which the HF dataset is split into 5 folds, each having a training and test set size of 80% and 20% of the data, respectively, and a validation set size of 10% of the training set in each fold (used for optimal epoch selection in case of neural models or hyperparameter selection in case of logistic regression). Moreover, due to the imbalance in outcome classes (i.e. no readmission vs. readmission), training examples were weighted inversely proportional to class/outcome frequencies in the training data. The models’ performance was evaluated using the last HF event in the patients’ timeline (i.e. 30 days all-cause readmission after hospitalization for HF event). We used the area under the ROC curve (AUC) as our performance measure with confidence intervals computed using the approach reported in LeDell et al. [42]. Moreover, the evaluation of the trained models was based on their average performance on the test sets of the five folds.

3.1 Hyperparameter optimization for neural models

Neural model hyperparameter selection is costly, particularly for finding the optimal architecture. To this end, we randomly chose one fold where 30% of the training set was further split into a training and validation set, each having 90% and 10% of the data, respectively. We developed a multiprocessing module that used a uniform random search strategy [43] that randomly chose a set of hyperparameters configurations (i.e. layer depth, filter size and optimization methods, see supplementary materials for more details) from the set of all possible configurations. Then the best configuration for each model (i.e. the one achieving best performance on the validation set) was used for the final training and testing.

4 Results

The HF dataset included 272,778 patients (49% female) with a mean (SD) age of 72.89 years (14). The total number of HF admissions was 343,328 (66.9% of all admissions) of which 81,087 (23.6%) were 30 days all-cause readmissions, corresponding to the official rates published by HCUP [2]. Among the last HF hospitalizations in patients’ timelines, 45,183 (16.6%) resulted in readmissions. Table 1 reports a general overview of the characteristics of the dataset including socio-demographics, hospitalization events, top diagnosis and procedures and the payment source. Table 2 reports the models’ performance in predicting the 30 days all-cause readmission for the last HF event in every patient’s timeline. Starting from RNN, the models trained with losses incorporating/emphasizing the loss from last HF event (i.e LastHF and Convex_HF_LastHF) achieved higher performance 0.636 and 0.635 AUC respectively compared to other loss definitions. Moreover, RNN models with all four loss definitions achieved higher performance than RNNSS counterparts. For models incorporating CRF, the RNNCRF model achieved the highest performance with 0.642, followed by Neural CRF 0.634 and CRF only model achieving 0.63 with the first two models using pairwise potentials and the last one using unary potential. For convolutional models, CNN-Wide achieved better performance 0.632 compared to

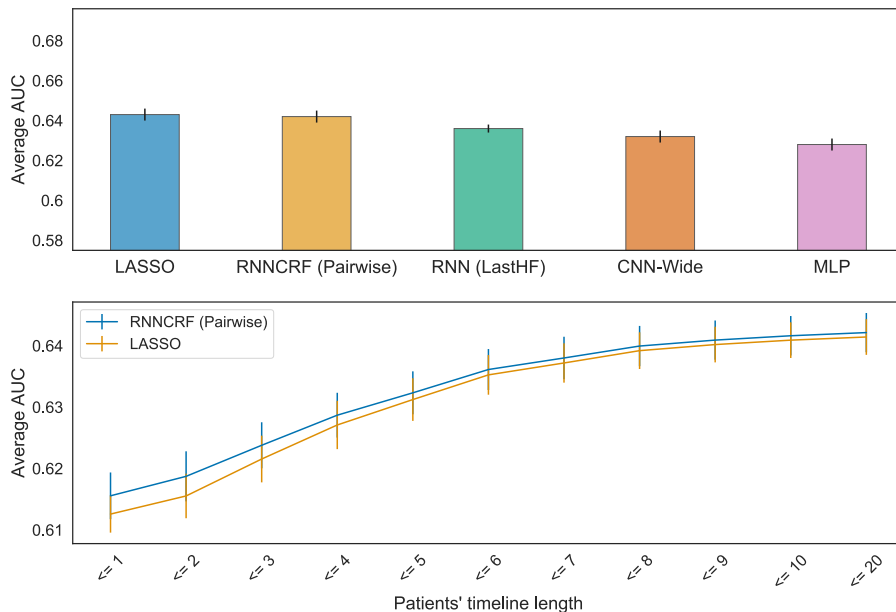


Figure 2: Ranking of best models (upper panel). Performance of LASSO versus RNNCRF model as function of patients' timeline length (lower panel)

conventional CNN with 0.619. The MLP model achieved 0.628 placing it as the lowest performing model among the classes of neural models (see Figure 2 top panel). The baseline model LR with l_1 -norm regularization (LASSO) achieved higher performance 0.643 compared to LR with l_2 -norm regularization 0.637. The ranking of the best performing models is depicted in Figure 2 where the bottom panel compares the performance of the LASSO to the RNNCRF model as a function of the length of patients' timeline. As the length of the timeline increases (i.e. more hospitalization events), the gap in last HF event prediction performance between both models decreases. The analysis of feature importance is reported in Figure 3, which shows the normalized coefficients of the trained LASSO models averaged across all folds. For the best neural model (RNNCRF), we report the analysis of feature importance using a similar approach to the one in [44]. In short, we iterated over all features attached to the last HF event, and computed the probability of readmission with a feature present or absent. Computing the difference between both probabilities allowed us to quantify a feature's importance across the five folds. In the supplementary material section, we present additional variations on this technique. Overall, the average overlap (using Jaccard similarity) of the top-100 features between LASSO and the RNNCRF model is 51% and 55% for increase and decrease of readmission probability, respectively.

Variables	HF Dataset (n=272,778)
Socio-demographics	
Age, mean (SD)	72.89 (14)
Gender female, count (%)	133765 (49%)
Pay source, count (%)	
Medicare	391535 (76.4%)
Private insurance	47327 (9.23%)
Medicaid	47095 (9.19%)
Self-pay	13115 (2.55%)
Other	11859 (2.31%)
No charge	1514 (0.29%)
Hospitalization events	
HF events, count (%)	343328 (66.94%)
30 days all-cause readmission, count (%)	81087 (23.61%)
Timeline length, mean (SD)	1.88 (1.4)
Top 5 diagnosis, count (%)	
Congestive heart failure; non-hypertensive	777047 (10.29%)
Coronary atherosclerosis and other heart disease	547890 (7.25%)
Residual codes	305406 (4.04%)
Cardiac dysrhythmias	298823 (3.95%)
Chronic kidney disease	254593 (3.37%)
Top 5 procedures, count (%)	
Diagnostic cardiac catheterization; coronary arteriography	106428 (14.95%)
Respiratory intubation and mechanical ventilation	57202 (8.03%)
Blood transfusion	52251 (7.34%)
Diagnostic ultrasound of heart (echocardiogram)	41076 (5.77%)
Hemodialysis	38083 (5.35%)

Table 1: Overview of HF dataset

Model name	AUC	CI - low	CI - high
CNN	0.619	0.616	0.622
CNN-Wide	0.632	0.629	0.635
RNN (Convex_HF_lastHF)	0.635	0.632	0.638
RNN (LastHF)	0.636	0.633	0.638
RNN (Uniform_HF)	0.631	0.628	0.634
RNN (Convex_HF_NonHF)	0.627	0.624	0.630
RNNSS (Convex_HF_lastHF)	0.621	0.618	0.624
RNNSS (LastHF)	0.625	0.623	0.628
RNNSS (Uniform_HF)	0.617	0.614	0.619
RNNSS (Convex_HF_NonHF)	0.625	0.622	0.628
Neural CRF (Pairwise)	0.634	0.631	0.637
Neural CRF (Unary)	0.631	0.629	0.634
CRF Only (Pairwise)	0.628	0.625	0.631
CRF Only (Unary)	0.630	0.627	0.633
RNNCRF (Pairwise)	0.642	0.640	0.645
RNNCRF (Unary)	0.638	0.635	0.641
MLP	0.628	0.625	0.631
Logistic regression (L2 reg.)	0.637	0.634	0.640
Logistic regression (L1 reg.)	0.643	0.640	0.646

Table 2: AUC models' performance

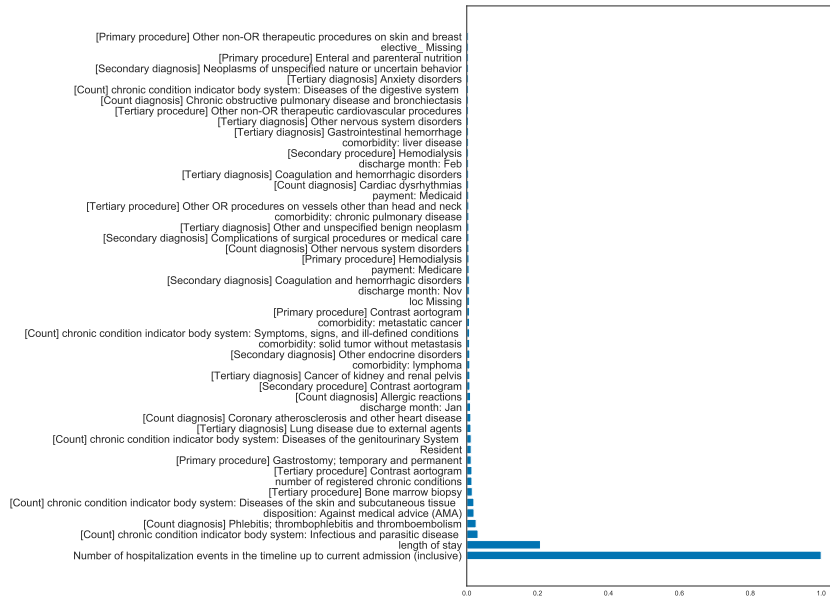


Figure 3: Top-50 features in LASSO models contributing to the increase of log-odds of readmission

5 Discussion

This work highlights the advantages and limitations of deep learning in the domain of HF readmission prediction. As a first result, we observe that deep learning profits from the incorporation of patients’ timeline / historical data for improving prediction performance. Particularly, sequence labeling (RNN, RN-NCRF, CRF only, Neural CRF) and sequence classification (CNN-Wide) overall perform better than event (non-timeline) classification (MLP). This finding is noteworthy, as it reflects the ability of deep learning, with the help of fast and highly specialized hardware and software, to utilize vast data resources to produce increasingly state-of-the-art machine learning performances. In the medical field, this amounts to a unique opportunity to allow machines to base their predictions not only on the current status of a patient, but also on the patient’s history, and, if possible, on the comparative analysis to all patient data (present and historical) in a hospital system. Our data supports this notion, showing that the detailed past history, reflected in a timeline of patient hospitalization events, indeed carries additional information that boosts deep learning prediction performance. Not all neural models are born equal though, and for our study, we find that a scheduled sampling approach for RNN did not improve timeline-based predictions. Interestingly, pairing the RNN with a graphical model (CRF) resulted in the best performing neural model, an observation that mirrors previous results in the field of NLP [30, 31]. Similarly, neural CRF performed better than CRF alone, hinting at the importance of adding nonlinear features to graphical models. While the actual performance numbers, with a maximal ROC score of 0.642 AUC (95% CI, 0.640-0.645), are inline with published machine-learning predictions of HF readmission [8, 9], it should be noted that they are based on administrative data, rather than rich EHR data as used in earlier studies. As such, our numbers represent the lower bound of achievable performance and deep learning on EHR data may eventually beat existing performance numbers for readmission prediction, as it did in other areas such as diagnosis and disease prediction [26, 45]. Nevertheless, the exact approach for attaining better performance remains an open research question. One obvious avenue is to use multi-modal learning, incorporating several clinical data sources (including images), to offset the inherent issues with textual medical data, such as sparsity, missingness, and incompleteness. Our second result addresses the question of deep learning versus logistic regression for readmission prediction. Our face-off shows that logistic regression with regularization matches the best neural network performance. Our study attempted to compare these two approaches as fairly as possible, allowing both methods to perform hyperparameter optimization in the training phase, and giving logistic regression, which uses data from the last hospitalization event only, access to a patient’s hospitalization history by adding timeline summary data as an additional feature of the hospitalization event. Nevertheless, the LASSO model had a couple of advantages over the neural models by (1) having access to the whole training set during the hyperparameter optimization, and (2) using l_1 -norm regularization that served as feature-selection procedure while training the model. In contrast, the neural-based models had a very large set of hyperparameters to choose from (such as number of layers, dimensions of hidden vectors, etc.) that made it infeasible to explore the full hyperparameter space. We therefore opted for a random selection process for network configurations

and optimization settings, and tested those against a subset of the training data only. Interestingly, and supporting our results, research by Rajkomar et al. [46] on a more general hospital readmission problem (not focused on HF) also showed that logistic regression with regularization (LASSO) is competitive compared to an RNN model. Focusing on neural models, we show that data contained in a patient’s history boost prediction performance. Particularly, neural models showed higher performance with the length of a patient’s timeline. EHRs contain historical information spanning several decades, and we will test in future studies whether deep learning on timelines greater than 11 month (the maximum used in this study) will succeed in besting the performance of logistic regression model. Finally, our study sheds light on which features from the current or past hospitalizations are essential in readmission prediction. Features such as number of hospitalization events, length of stay, thrombophlebitis/thromboembolism and discharge against medical advice are among the highest contributing features to the log-odds of readmission. Generally, diagnoses and administered procedures pertaining to heart problems, such as contrast aortograms, result in increased readmission probability, as does the number of comorbidities. Interestingly, particular payment sources (Medicare and Medicaid) are associated with increased, while self-pay is associated with decreased readmissions.

In conclusion, we show that neural network models and logistic regression have comparable performance on HF readmission prediction using administrative data. We also demonstrate that the use of patient timeline data boosts the performance of neural models.

Availability

The data processing, model implementation, training and testing workflow in addition to the trained models are publicly available at https://bitbucket.org/A_2/hcup_research

Acknowledgements

We would like to thank Dr. Harlan Krumholz for his insights and discussions about the research topic.

Competing Interests

None.

Funding

AA was supported by a fellowship from the Intramural Research Program of the National Institutes of Health (NIH), National Library of Medicine (NLM), and Lister Hill National Center for Biomedical Communications (LHNCBC).

Contributions

AA and MK conceptualized and designed the experiments. MN and GT contributed in the design of the experiments. MK and GT supervised the project. AA worked on the development of processing and analysis workflow, algorithms and model implementation. MN contributed in the analysis workflow. AA and MK analyzed and interpreted the data. AA and MK wrote the manuscript.

6 References

- [1] Fingar, K. & Washington, R. Trends in Hospital Readmissions for Four High-Volume Conditions, 2009-2013: Statistical Brief #196. *HCUP Statistical Brief #196* 1–17 (2006).
- [2] Fingar, K. R., Barrett, M. L. & Jiang, H. J. A Comparison of All-Cause 7-Day and 30-Day Readmissions, 2014. *HCUP Statistical Brief #230* (2017).
- [3] Bergethon, K. E. *et al.* Trends in 30-Day Readmission Rates for Patients Hospitalized with Heart Failure: Findings from the Get with the Guidelines-Heart Failure Registry. *Circulation: Heart Failure* **9**, e002594 (2016). 15334406.
- [4] Desai, A. S. & Stevenson, L. W. Rehospitalization for Heart Failure. *Circulation* **126**, 501–506 (2012).
- [5] Ross, J. S. *et al.* Recent National Trends in Readmission Rates after Heart Failure Hospitalization. *Circulation: Heart Failure* (2009).
- [6] Arundel, C. *et al.* Association of 30-Day All-Cause Readmission with Long-Term Outcomes in Hospitalized Older Medicare Beneficiaries with Heart Failure. *American Journal of Medicine* **129**, 1178–1184 (2016).
- [7] Ziaeeian, B. & Fonarow, G. C. The Prevention of Hospital Readmissions in Heart Failure. *Progress in Cardiovascular Diseases* **58**, 379–385 (2016).
- [8] Mortazavi, B. J. *et al.* Analysis of Machine Learning Techniques for Heart Failure Readmissions. *Circulation: Cardiovascular Quality and Outcomes* **9**, 629–640 (2016).
- [9] Frizzell, J. D. *et al.* Prediction of 30-Day All-Cause Readmissions in Patients Hospitalized for Heart Failure. *JAMA Cardiology* **2**, 204 (2017).
- [10] HCUP Databases. HCUP Nationwide Readmission Database (NRD). Healthcare Cost and Utilization Project (HCUP). Agency for Healthcare Research and Quality (2013).
- [11] HCUP Nationwide Readmission Databaset (NRD). Description of Data Elements.
- [12] HCUP Software. HCUP Clinical Classifications Software (CCS) for ICD-9-CM (2009).
- [13] HCUP Software. HCUP Chronic Condition Indicator (CCI) (2009).
- [14] HCUP Software. HCUP Comorbidity Software (2008).
- [15] Barrett, M., Raetzman, S. & Andrews, R. HCUP Methods Series Overview of Key Readmission Measures and Methods Report # 2012-04. Tech. Rep., U.S. Agency for Healthcare Research and Quality (2012).
- [16] Elman, J. L. Finding Structure in Time. *Cognitive Science* **14**, 179–211 (1990).

- [17] Graves, A. *Supervised Sequence Labelling with Recurrent Neural Networks*, vol. 385 of *Studies in Computational Intelligence* (Springer Berlin Heidelberg, Berlin, Heidelberg, 2012).
- [18] Lipton, Z. C., Berkowitz, J. & Elkan, C. A Critical Review of Recurrent Neural Networks for Sequence Learning (2015). 1506.00019.
- [19] Werbos, P. Backpropagation through time: what it does and how to do it. *Proceedings of the IEEE* **78**, 1550–1560 (1990).
- [20] Hochreiter, S. *Untersuchungen zu dynamischen neuronalen Netzen*. Diploma thesis, Technische Universität München (1991).
- [21] Bengio, Y., Simard, P. & Frasconi, P. Learning long-term dependencies with gradient descent is difficult. *IEEE Transactions on Neural Networks* **5**, 157–166 (1994).
- [22] Pascanu, R., Mikolov, T. & Bengio, Y. On the difficulty of training recurrent neural networks. In *Proceedings of the 30th International Conference on Machine Learning* (JMLR: W&CP volume 28, Atlanta, Georgia, 2013).
- [23] Hochreiter, S. & Schmidhuber, J. Long Short-Term Memory. *Neural Computation* **9**, 1735–1780 (1997).
- [24] Cho, K. *et al.* Learning Phrase Representations using RNN Encoder-Decoder for Statistical Machine Translation. In *Proceedings of the 2014 Conference on Empirical Methods in Natural Language Processing (EMNLP)*, 1724–1734 (Association for Computational Linguistics, Doha, Qatar, 2014).
- [25] Chung, J., Gulcehre, C., Cho, K. & Bengio, Y. Empirical Evaluation of Gated Recurrent Neural Networks on Sequence Modeling (2014). 1412.3555.
- [26] Lipton, Z. C., Kale, D. C., Elkan, C. & Wetzell, R. Learning to Diagnose with LSTM Recurrent Neural Networks (2015). 1511.03677.
- [27] Srivastava, N., Hinton, G., Krizhevsky, A., Sutskever, I. & Salakhutdinov, R. Dropout: A Simple Way to Prevent Neural Networks from Overfitting. *Journal of Machine Learning Research* **15**, 1929–1958 (2014).
- [28] Bengio, S., Vinyals, O., Jaitly, N. & Shazeer, N. Scheduled Sampling for Sequence Prediction with Recurrent Neural Networks. In Cortes, C., Lawrence, N. D., Lee, D. D., Sugiyama, M. & Garnett, R. (eds.) *Advances in Neural Information Processing Systems 28*, 1171–1179 (Curran Associates, Inc., 2015).
- [29] Lafferty, J., McCallum, A. & Pereira, F. C. N. Conditional random fields: Probabilistic models for segmenting and labeling sequence data. *ICML '01 Proceedings of the Eighteenth International Conference on Machine Learning* **8**, 282–289 (2001). arXiv:1011.4088v1.
- [30] Lample, G., Ballesteros, M., Subramanian, S., Kawakami, K. & Dyer, C. Neural Architectures for Named Entity Recognition (2016). 1603.01360.

- [31] Ma, X. & Hovy, E. End-to-end Sequence Labeling via Bi-directional LSTM-CNNs-CRF. In *Proceedings of the 54th Annual Meeting of the Association for Computational Linguistics*, 1064–1074 (Association for Computational Linguistic, Berlin, Germany, 2016).
- [32] Peng, J., Bo, L. & Xu, J. Conditional neural fields. In Bengio, Y., Schuurmans, D., Lafferty, J. D., Williams, C. K. I. & Culotta, A. (eds.) *Advances in Neural Information Processing Systems 22*, 1419–1427 (Curran Associates, Inc., 2009).
- [33] Bishop, C. M. *Pattern recognition and machine learning* (Springer, 2006).
- [34] Viterbi, A. Error bounds for convolutional codes and an asymptotically optimum decoding algorithm. *IEEE Transactions on Information Theory* **13**, 260–269 (1967).
- [35] Collins, M. Log-Linear Models, MEMMs, and CRFs.
- [36] Ye, N., Lee, W. S., Chieu, H. L. & Wu, D. Conditional Random Fields with High-Order Features for Sequence Labeling. *Neural Information Processing Systems* **2**, 2 (2009).
- [37] Cuong, N. V., Ye, N., Lee, W. S. & Chieu, H. L. Conditional Random Field with High-order Dependencies for Sequence Labeling and Segmentation. *Journal of Machine Learning Research* **15**, 981–1009 (2014).
- [38] Vieira, T., Cotterell, R. & Eisner, J. Speed-Accuracy Tradeoffs in Tagging with Variable-Order CRFs and Structured Sparsity. In *Emnlp*, 1973–1978 (Association for Computational Linguistics, Austin, Texas, 2016).
- [39] Allam, A. & Krauthammer, M. PySeqLab: an open source Python package for sequence labeling and segmentation. *Bioinformatics* **33**, 3497–3499 (2017).
- [40] Simonyan, K. & Zisserman, A. Very Deep Convolutional Networks for Large-Scale Image Recognition. In *ICLR* (2015). [arXiv:1409.1556v6](https://arxiv.org/abs/1409.1556v6).
- [41] Kim, Y. Convolutional Neural Networks for Sentence Classification. In *EMNLP*, 1746–1751 (Association for Computational Linguistics, 2014).
- [42] LeDell, E., Petersen, M. & van der Laan, M. Computationally efficient confidence intervals for cross-validated area under the ROC curve estimates. *Electronic Journal of Statistics* **9**, 1583–1607 (2015).
- [43] Bergstra JAMESBERGSTR, J. & Yoshua Bengio YOSHUABENGIO, U. Random Search for HyperParameter Optimization. *Journal of Machine Learning Research* (2012). [1504.05070](https://arxiv.org/abs/1504.05070).
- [44] Avati, A. *et al.* Improving palliative care with deep learning. In *2017 IEEE International Conference on Bioinformatics and Biomedicine (BIBM)*, 311–316 (IEEE, 2017).
- [45] Choi, E., Schuetz, A., Stewart, W. F. & Sun, J. Using recurrent neural network models for early detection of heart failure onset. *Journal of the American Medical Informatics Association* **24**, 361–370 (2017).

- [46] Rajkomar, A. *et al.* Scalable and accurate deep learning with electronic health records. *npj Digital Medicine* **1**, 18 (2018).

Supplementary Material for Neural networks versus Logistic regression for 30 days all-cause readmission prediction

A Methods

A.1 Recurrent neural network (RNN)

RNN computes a hidden vector at each time step (i.e. state vector \bar{h}_t at time t), representing a history or context summary of the sequence using the input and hidden states vector from the previous time step. This allows the model to learn long-range dependencies where the network is unfolded as many times as the length of the sequence it is modeling. Equation 6 shows the computation of the hidden vector \bar{h}_t using the input \bar{x}_t and the previous hidden vector \bar{h}_{t-1} where ϕ is a non-linear transformation such as $ReLU(z) = \max(0, z)$ or $\tanh(z) = \frac{e^z - e^{-z}}{e^z + e^{-z}}$. To compute the outcome \hat{y}_t at time t , an affine transformation followed by non-linear function are applied to the state vector \bar{h}_t as described in Equation 7. The non-linear operator σ can be either the *sigmoid* function $\sigma(z) = \frac{1}{1+e^{-z}}$ applied to scalar input $z \in \mathbb{R}$, or its generalization the *softmax* function applied to vector $\bar{z} \in \mathbb{R}^K$, $\text{softmax}(\bar{z})_i = \frac{e^{\bar{z}_i}}{\sum_{j=1}^K e^{\bar{z}_j}}$ for $i = 1, \dots, K$. As a result, the outcome \hat{y}_t represents a probability distribution over the set of possible labels V_{label} at time t .

$$\bar{h}_t = \phi(\mathbf{W}_{hx}\bar{x}_t + \mathbf{W}_{hh}\bar{h}_{t-1} + \bar{b}_{hx}) \quad (6)$$

$$\hat{y}_t = \sigma(\mathbf{W}_{V_{label}h}\bar{h}_t + \bar{b}_{V_{label}}) \quad (7)$$

where $\mathbf{W}_{hh} \in \mathbb{R}^{D_h \times D_h}$, $\mathbf{W}_{hx} \in \mathbb{R}^{D_h \times d}$, $\mathbf{W}_{V_{label}h} \in \mathbb{R}^{|V_{label}| \times D_h}$, $\bar{b}_{hx} \in \mathbb{R}^{D_h}$, $\bar{b}_{V_{label}} \in \mathbb{R}^{|V_{label}|}$ representing the model weights θ to be optimized and D_h , d are the dimensions of \bar{h}_t and \bar{x}_t vectors respectively. Note that the weights are shared across all the network (see Figure 4 for RNN representation).

A.1.1 Long short-term memory (LSTM)

Long short-term memory (LSTM) [17, 23] falls in the gated memory cells approach that modifies the basic RNN by replacing the standard neurons/units in the hidden layer with gated/memory cells to generate the hidden state vector \bar{h}_t as described by the equations below. Moreover, LSTM introduces a new cell state vector \bar{c}_t that overall contributes in the decision mechanism on what part of the history to keep or forget. The computation of the output \hat{y}_t at time t remains the same as explained in the RNN section.

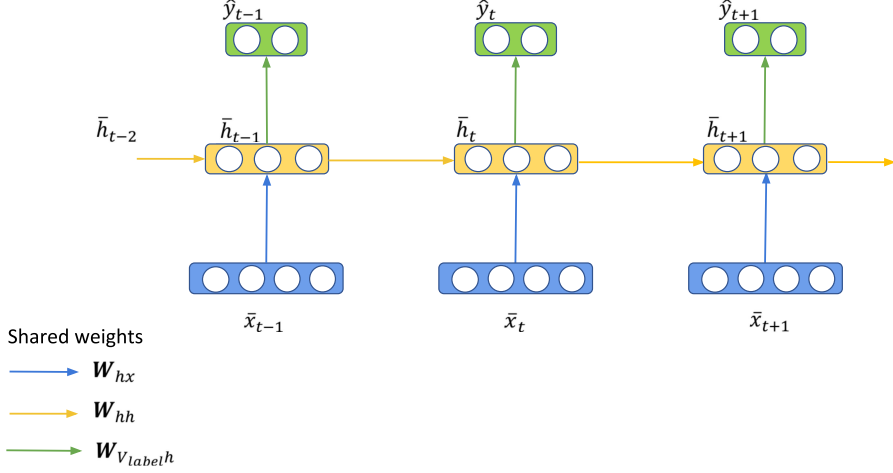


Figure 4: Graphical representation of unfolded RNN

$$\begin{aligned}
 \bar{i}_t &= \sigma(\mathbf{W}_{hx}^i \bar{x}_t + \mathbf{W}_{hh}^i \bar{h}_{t-1} + \bar{b}_{hx}^i) && \text{(input gate)} \\
 \bar{f}_t &= \sigma(\mathbf{W}_{hx}^f \bar{x}_t + \mathbf{W}_{hh}^f \bar{h}_{t-1} + \bar{b}_{hx}^f) && \text{(forget gate)} \\
 \bar{o}_t &= \sigma(\mathbf{W}_{hx}^o \bar{x}_t + \mathbf{W}_{hh}^o \bar{h}_{t-1} + \bar{b}_{hx}^o) && \text{(output gate)} \\
 \bar{c}_t &= \phi(\mathbf{W}_{hx}^{\bar{c}} \bar{x}_t + \mathbf{W}_{hh}^{\bar{c}} \bar{h}_{t-1} + \bar{b}_{hx}^{\bar{c}}) && \text{(new state/memory cell)} \\
 \bar{c}_t &= \bar{f}_t \odot \bar{c}_{t-1} + \bar{i}_t \odot \bar{c}_t && \text{(final cell state)} \\
 \bar{h}_t &= \bar{o}_t \odot \phi(\bar{c}_t) && \text{(hidden state vector)}
 \end{aligned}$$

where \mathbf{W}_{hx}^i , \mathbf{W}_{hx}^f , \mathbf{W}_{hx}^o , $\mathbf{W}_{hx}^{\bar{c}}$ each $\in \mathbb{R}^{D_h \times d}$ and \mathbf{W}_{hh}^i , \mathbf{W}_{hh}^f , \mathbf{W}_{hh}^o , $\mathbf{W}_{hh}^{\bar{c}}$ each $\in \mathbb{R}^{D_h \times D_h}$. The biases \bar{b}_{hx}^i , \bar{b}_{hx}^f , \bar{b}_{hx}^o , $\bar{b}_{hx}^{\bar{c}}$ each $\in \mathbb{R}^{D_h}$ where D_h and d are the dimensions of \bar{h}_t and \bar{x}_t vectors respectively. The operator σ represents the *sigmoid* function, ϕ the *tanh* or *ReLU* function, and \odot the element-wise product (i.e. Hadamard product) function. Compared to the standard/conventional RNN (see Equation 6), it can be noted the added complexity in terms of the number of weight matrices and biases required to compute the hidden state vector \bar{h}_t .

A.1.2 Gated recurrent unit (GRU)

Gated recurrent unit (GRU) [24] presents similar approach to LSTM but with a simpler model that modifies the computation mechanism of the hidden state vector \bar{h}_t through the specified equations below.

$$\begin{aligned}
\bar{z}_t &= \sigma(\mathbf{W}_{hx}^z \bar{x}_t + \mathbf{W}_{hh}^z \bar{h}_{t-1} + \bar{b}_{hx}^z) && \text{(update gate)} \\
\bar{r}_t &= \sigma(\mathbf{W}_{hx}^r \bar{x}_t + \mathbf{W}_{hh}^r \bar{h}_{t-1} + \bar{b}_{hx}^r) && \text{(reset gate)} \\
\bar{\tilde{h}}_t &= \phi(\mathbf{W}_{hx}^{\tilde{h}} \bar{x}_t + \bar{r}_t \odot \mathbf{W}_{hh}^{\tilde{h}} \bar{h}_{t-1} + \bar{b}_{hx}^{\tilde{h}}) && \text{(new state/memory cell)} \\
\bar{h}_t &= (1 - \bar{z}_t) \odot \bar{\tilde{h}}_t + z_t \odot h_{t-1} && \text{(hidden state vector)}
\end{aligned}$$

The model computes a reset gate \bar{r}_t that is used to modulate the effect of the previous hidden state vector \bar{h}_{t-1} when computing the new memory vector $\bar{\tilde{h}}_t$. The update gate \bar{z}_t determines the importance/contribution of the newly generated memory vector $\bar{\tilde{h}}_t$ compared to the previous hidden state vector \bar{h}_{t-1} when computing the current hidden vector \bar{h}_t . The weights \mathbf{W}_{hx}^z , \mathbf{W}_{hx}^r , $\mathbf{W}_{hx}^{\tilde{h}}$ each $\in \mathbb{R}^{D_h \times d}$ and \mathbf{W}_{hh}^z , \mathbf{W}_{hh}^r , $\mathbf{W}_{hh}^{\tilde{h}}$ each $\in \mathbb{R}^{D_h \times D_h}$. The biases \bar{b}_{hx}^z , \bar{b}_{hx}^r , $\bar{b}_{hx}^{\tilde{h}}$ each $\in \mathbb{R}^{D_h}$ where D_h and d are the dimensions of \bar{h}_t and \bar{x}_t vectors respectively. The operators notation have the same meaning as described in the LSTM section.

A.1.3 RNN objective function

In our work, we use RNN to refer to RNN, LSTM and GRU models targeting the sequence labeling view of the problem. We defined the loss for an i -th sequence at each time step by the cross-entropy error

$$l_t^{(i)} = - \sum_{c=1}^{|\text{Vlabel}|} y_{t,c}^{(i)} \times \log(\hat{y}_{t,c}^{(i)}) \quad (8)$$

where the loss for the i -th sequence (i.e. i -th patient's timeline/trajectory) is defined by the average loss over the sequence length T_i

$$L_i = \frac{1}{T_i} \sum_{t=1}^{T_i} l_t^{(i)} \quad (9)$$

Given that our focus is on the 30 days all-cause readmissions after HF hospitalization, our model's focus should be on the index events (i.e. claims/events where HF is the primary diagnosis of hospitalization). Hence, the objective function could be modified to reflect this requirement. We modify the defined loss over i -th sequence (see Equation 9) by defining an average loss for non-index and index events separately and then taking a convex combination between both losses parametrized by α . The parameter α is determined using a validation set. Our modification is inspired by the work done in [26].

$$\begin{aligned}
L_i^{HF} &= \frac{1}{\sum_{t=1}^{T_i} \mathbb{1}[\bar{x}_{t,primaryHF}^{(i)} = 1]} \sum_{t=1}^{T_i} l_t^{(i)} \mathbb{1}[\bar{x}_{t,primaryHF}^{(i)} = 1] \\
L_i^{nonHF} &= \frac{1}{\sum_{t=1}^{T_i} \mathbb{1}[\bar{x}_{t,primaryHF}^{(i)} = 0]} \sum_{t=1}^{T_i} l_t^{(i)} \mathbb{1}[\bar{x}_{t,primaryHF}^{(i)} = 0]
\end{aligned}$$

$$L_i = (1 - \alpha)L_i^{nonHF} + \alpha(L_i^{HF}) \quad (10)$$

where $\mathbb{1}[\bar{x}_{t,primaryHF}^{(i)} = 1]$ is an indicator function that is equal to 1 when the feature vector $\bar{x}_t^{(i)}$ representing the event at time t for the i -th sequence has HF as the primary diagnosis (we refer to this loss by Convex_HF_NonHF). A second variation (Uniform_HF) to the first objective function in Equation 10, is to consider only the index events in the patients' timeline where we compute the average cross-entropy loss for the index events only.

$$L_i = L_i^{HF} \quad (11)$$

A third variation (Convex_HF_lastHF) is to take a convex combination between all index events and the last index event in the timeline.

$$L_i^{HF} = \frac{1}{\sum_{t=1}^{T_i} \mathbb{1}[\bar{x}_{t,primaryHF}^{(i)} = 1]} \sum_{t=1}^{T_i} l_t^{(i)} \mathbb{1}[\bar{x}_{t,primaryHF}^{(i)} = 1]$$

$$L_i^{lastHF} = l_T^{(i)}$$

$$L_i = (1 - \alpha)L_i^{HF} + \alpha(L_i^{lastHF}) \quad (12)$$

where L_i^{lastHF} is the cross-entropy loss for the last HF event (i.e. the last index event in the patient's timeline) and $l_T^{(i)} = -\sum_{c=1}^{V_{label}} y_{T,c}^{(i)} \times \log(\hat{y}_{T,c}^{(i)})$. The previous variations consider the *sequence labeling* approach since the loss function for a sequence is defined as a composite of losses from different times/events in a patient's timeline. A final variation that uses the *sequence classification* view of the problem is to define an objective function that focuses only on the last HF event (LastHF) by computing the loss at the last target event we aim to predict.

$$L_i = L_i^{lastHF} \quad (13)$$

Lastly, the objective function for the whole training set D_{train} is defined by the average loss across all the sequences in D_{train} plus a weight regularization term (i.e. l_2 -norm regularization) applied to the model parameters represented by θ

$$L(\theta) = \frac{1}{N} \sum_{i=1}^N L_i + \frac{\lambda}{2} \|\theta\|_2^2 \quad (14)$$

In practice, the training occurs using mini-batches where computing the loss function and updating the parameters/weight occur after processing each mini-batch of the training set.

A.1.4 RNN with conditional random fields (CRF)

CRF models the conditional probability of a sequence \underline{y} given its corresponding sequence of observation vectors \underline{x} (i.e. $p(y_1, y_2, \dots, y_T | \bar{x}_1, \bar{x}_2, \dots, \bar{x}_T)$) using

a parametrized *global* feature vector $\overline{F}(\underline{\mathbf{x}}, \underline{\mathbf{y}}) \in \mathbb{R}^J$ that takes input/output sequences to produce J -dimensional vector. As a result, the computation of the conditional probability of an output sequence given its input sequence of observations is equal to

$$p(\underline{\mathbf{y}}|\underline{\mathbf{x}}) = \frac{e^{\boldsymbol{\theta} \cdot \overline{F}(\underline{\mathbf{x}}, \underline{\mathbf{y}})}}{\sum_{\underline{\mathbf{y}}' \in \mathbf{Y}} e^{\boldsymbol{\theta} \cdot \overline{F}(\underline{\mathbf{x}}, \underline{\mathbf{y}}')}} \quad (15)$$

where \mathbf{Y} is the set of all label sequences, the denominator represents the normalizer (commonly referred to the partition function Z), and $\boldsymbol{\theta}$ is the weight vector corresponding to the global feature vector $\overline{F}(\underline{\mathbf{x}}, \underline{\mathbf{y}})$. The common definition of the feature vector \overline{F} uses the first-order Markov assumption in order to make the inference and model training tractable [35]. That is

$$\overline{F}(\underline{\mathbf{x}}, \underline{\mathbf{y}}) = \sum_{t=1}^T \overline{f}(\underline{\mathbf{x}}, t, y_{t-1}, y_t) \quad (16)$$

where the global feature vector \overline{F} is the sum of a local feature vector \overline{f} applied at each time step until the end of the sequence. The local vector \overline{f} has the same dimension of \overline{F} (i.e. $\in \mathbb{R}^J$) and has access to the whole observation sequence $\underline{\mathbf{x}}$, and the current and previous states/outputs y_{t-1} and y_t [35]. Generally, increasing the model order k (i.e. $k \geq 2$) would lead to exponential computational complexity in terms of k . However, recent work as in [36–38], showed under the assumption of label pattern sparsity, the use of higher-order models (i.e. models with $k \geq 2$) is feasible without incurring an exponential complexity in the training and inference algorithms [39].

We denote the output features of the RNN layer by $\underline{\mathbf{z}} = [\bar{z}_1, \bar{z}_2, \dots, \bar{z}_T]$ representing the sequence of output features computed from the input sequence $\underline{\mathbf{x}}$ (both sequences have equal length). The potential functions in the CRF layer are computed using $\underline{\mathbf{z}}$ along with label sequence $\underline{\mathbf{y}}$. In our work, we experimented with two potential functions:

1. RNNCRF (Unary) that computes unary potentials $\psi_{y_t}(\bar{z}_t)$ by passing the RNN output feature vector \bar{z}_t at time t to a linear affine map and applying a non-linear transformation resulting in a vector of size equal to the number of classes $|V_{label}|$ for each \bar{z}_t . The pairwise potential is modeled using a transition parameters matrix $A(y_{t-1}, y_t)$ of size $|V_{label}| \times |V_{label}|$ representing the transition score from one outcome class to another. The total score computation is equal to $\overline{F}(\underline{\mathbf{z}}, \underline{\mathbf{y}}) = \sum_{t=1}^T (\psi_{y_t}(\bar{z}_t) + A(y_{t-1}, y_t))$.
2. RNNCRF (Pairwise) that computes pairwise potentials $\psi_{y_{t-1}y_t}(\bar{z}_t)$ by using linear affine map transformation followed by non-linear element-wise operation generating an output of size $|V_{label}| \times |V_{label}|$ similar to the approach reported in [31]. The total score $\overline{F}(\underline{\mathbf{z}}, \underline{\mathbf{y}})$ is equal to $\overline{F}(\underline{\mathbf{z}}, \underline{\mathbf{y}}) = \sum_{t=1}^T \psi_{y_{t-1}y_t}(\bar{z}_t)$.

A.2 Dataset features representation

A.2.1 Input features \bar{x}_t

Each claim/event in a patient’s timeline is represented by a feature vector \bar{x}_t encoding the characteristics of the hospitalization event and the corresponding patient. The feature vector \bar{x}_t is composed of:

- **Diagnosis:** every claim in the dataset includes 25 ordered fields, each registering patient’s diagnosis category based on CCS grouper [12] during the corresponding hospitalization event. We first extracted set $V_{diagnosis}$ representing the diagnosis having at least 1000 counts/occurrences registered in the HF dataset. Then, we constructed the following vectors:
 1. \bar{x}_{diag1} a one-hot encoded vector $\in \{0, 1\}^{|V_{diagnosis}|}$ representing the diagnosis category registered for the primary diagnosis field
 2. \bar{x}_{diag2} a one-hot encoded vector $\in \{0, 1\}^{|V_{diagnosis}|}$ representing the diagnosis category registered for the secondary diagnosis field
 3. \bar{x}_{diag3} a one-hot encoded vector $\in \{0, 1\}^{|V_{diagnosis}|}$ representing the diagnosis category registered for the tertiary diagnosis field
 4. $\bar{x}_{countdiag}$ a vector $\in \mathbb{R}^{|V_{diagnosis}|}$ representing the count of diagnosis categories registered in all 25 diagnosis fields
- **Procedures:** every claim in the dataset includes 15 ordered fields, each registering patient’s administered procedure category based on CCS grouper during the corresponding hospitalization event. We first extracted set $V_{procedures}$ representing the top procedures having at least 1000 counts registered in HF dataset. Then, we constructed the following vectors:
 1. \bar{x}_{proc1} a one-hot encoded vector $\in \{0, 1\}^{|V_{procedures}|}$ representing the procedure category registered for the primary procedure field
 2. \bar{x}_{proc2} a one-hot encoded vector $\in \{0, 1\}^{|V_{procedures}|}$ representing the procedure category registered for the secondary procedure field
 3. \bar{x}_{proc3} a one-hot encoded vector $\in \{0, 1\}^{|V_{procedures}|}$ representing the procedure category registered for the tertiary procedure field
 4. $\bar{x}_{countproc}$ a vector $\in \mathbb{R}^{|V_{procedures}|}$ representing the count of procedure categories registered in all 15 procedure fields
- **Body-system chronic condition:** every claim in the dataset includes 25 ordered fields, each representing body-system chronic condition indicators, categorizing ICD-9-CM diagnosis codes into chronic or not [13]. We refer to the list of body-system categories by set $V_{bchronic}$ that includes 18 categories. We constructed the following vectors:
 1. $\bar{x}_{bchronic1}$ a one-hot encoded vector $\in \{0, 1\}^{|V_{bchronic}|}$ representing the body-system chronic condition indicator category listed in the primary field
 2. $\bar{x}_{bchronic2}$ a one-hot encoded vector $\in \{0, 1\}^{|V_{bchronic}|}$ representing the body-system chronic condition indicator category listed in the secondary field

3. $\bar{x}_{bchronic3}$ a one-hot encoded vector $\in \{0, 1\}^{|V_{bchronic}|}$ representing the body-system chronic condition indicator category listed in the tertiary field
 4. $\bar{x}_{countbchronic}$ a vector $\in \mathbb{R}^{|V_{bchronic}|}$ representing the count of body-system chronic condition indicator categories registered in the 25 fields
- External cause of injury code: every claim in the dataset includes 4 ordered fields, each detailing an injury code (E-code) based on CCS software categorizing all ICD-9-CM diagnosis codes into 20 categories [13]. We refer to the list of E-code categories by set V_{ecode} that includes 20 categories. We constructed the following vectors:
 1. \bar{x}_{ecode1} a one-hot encoded vector $\in \{0, 1\}^{|V_{ecode}|}$ representing the E-code injury category listed in the primary field
 2. $\bar{x}_{countecode}$ a vector $\in \mathbb{R}^{|V_{ecode}|}$ representing the count of E-code injury categories registered in the 4 fields
 - Procedure classes: every claim in the dataset includes 15 ordered fields, each describing a broad category code (i.e. class) based on categorization of the ICD-9-CM procedure codes [13]. We refer to the list of procedure broad categories by set $V_{procedureclass}$ that includes 4 categories. We constructed the following vectors:
 1. $\bar{x}_{countpclass}$ a vector $\in \mathbb{R}^{|V_{procedureclass}|}$ representing the count of procedure class categories registered in the 15 fields
 - Comorbidity condition: every claim in the dataset includes 29 binary fields $\in \{0, 1\}$, each representing an indicator of a specific comorbidity that was determined by the AHRQ comorbidity software [14]. The software determines comorbidities that are more likely present prior to hospitalization event [14]. We refer to the comorbidity categories encoded in the 29 binary variables by set $V_{comorbid}$. We constructed the following vector:
 1. $\bar{x}_{comorbid}$ a vector $\in \{0, 1\}^{|V_{comorbid}|}$ where each component corresponds to one of the 29 binary fields representing the presence/absence of a comorbidity condition
 - Major diagnostic category (MDC) assigned by HCFA DRG Grouper algorithm during the processing of HCUP dataset [13]. We refer to the list of MDC categories by set V_{mdc} where we constructed the following vector:
 1. \bar{x}_{mdc} a one-hot encoded vector $\in \{0, 1\}^{|V_{mdc}|}$ representing the MDC code/category
 - Risk of mortality subclass: every claim in the dataset includes a field that measures risk of mortality subclass based on all patient refined diagnosis related groups assigned using software developed by 3M Health Information System [13]. The measure consists of five categories which we refer to by the set $V_{riskmortal}$. We constructed the following vector:
 1. $\bar{x}_{riskmortal}$ a one-hot encoded vector $\in \{0, 1\}^{|V_{riskmortal}|}$ representing the risk of mortality subclass category

- Severity of illness subclass: every claim in the dataset includes a field that measures severity of illness subclass based on all patient refined diagnosis related groups assigned using software developed by 3M Health Information System [13]. The measure consists of five categories which we refer to set $V_{severity}$. We constructed the following vector:
 1. $\bar{x}_{severity}$ a one-hot encoded vector $\in \{0, 1\}^{|V_{severity}|}$ representing the severity of illness subclass category
- Major operating room procedure indicator: $x_{orproc} \in \{0, 1\}$ a binary variable indicating whether a major operating room procedure was reported on discharge
- Number of chronic conditions: $x_{chronic} \in \mathbb{R}$ a variable representing the counts of unique chronic diagnosis reported on the discharge
- Socio-demographics: every claim is associated with a patient and includes information regarding patient’s age, gender, income and place/location of residence. We constructed a vector $\bar{x}_{sociodem}$ that represents the concatenation of the following variables:
 1. age: $x_{age} \in \mathbb{R}$ a variable representing the age of the patient
 2. gender: $x_{gender} \in \{0, 1\}$ a binary variable representing the gender of a patient
 3. income: $\bar{x}_{income} \in \{0, 1\}^{|V_{income}|}$ a one-hot encoded vector indicating the median household income quartile for patient’s zip code, where V_{income} is the set of income categories
 4. place/location: $\bar{x}_{ploc} \in \{0, 1\}^{|V_{ploc}|}$ a one-hot encoded vector describing patient’s location based on the National Center for Health Statistics (NCHS) classification scheme for US counties, where V_{ploc} is the set of location categories
 5. resident: $x_{resident} \in \{0, 1\}$ a binary variable representing if the patient is resident in the state in which they were treated
- Event/claim info: every claim included the length of stay of the hospitalization event, if the admission was on a weekend, and the discharge month. We also computed the time difference between the hospital admission of a current claim/event and the discharge of previous claim/event for all events in a patient’s timeline. We constructed a vector \bar{x}_{event} that is the concatenation of the following variables:
 1. length of stay: $x_{los} \in \mathbb{R}$ a variable representing the length of stay in days for each hospitalization event
 2. time difference between consecutive events: $x_{\Delta t} \in \mathbb{R}$ a variable representing the time difference in days between current admission and previous discharge events
 3. admission on weekend: $x_{awweekend} \in \{0, 1\}$ a binary variable indicating if a patient was admitted on a weekend
 4. discharge month: $\bar{x}_{dmonth} \in \{0, 1\}^{|V_{dmonth}|}$ a one-hot encoded vector indicating a patient’s discharge month where V_{dmonth} is the set of recorded months in the dataset

5. disposition of patient: $\bar{x}_{dispuniform} \in \{0, 1\}^{|\mathcal{V}_{dispuniform}|}$ a one-hot encoded vector indicating the disposition of the patient at discharge
6. expected primary payer: $\bar{x}_{paysrc} \in \{0, 1\}^{|\mathcal{V}_{paysrc}|}$ a one-hot encoded vector indicating the expected primary payer (such as Medicare, private insurance, etc.)
7. same-day event: $\bar{x}_{sameday} \in \{0, 1\}^{|\mathcal{V}_{sameday}|}$ a one-hot encoded vector identifying transfers and/or same-day stay collapsed records
8. elective admission: $x_{elective} \in \{0, 1\}$ a binary variable indicating elective versus non-elective admission
9. rehab transfer: $x_{rehab} \in \{0, 1\}$ a binary variable indicating if the claim is a combined record involving transfer to rehabilitation, evaluation, or other aftercare
10. number of index events: $x_{countindex} \in \mathbb{R}$ a variable representing the number of index events in the timeline of a patient up to the current admission event (inclusive)
11. number of admission events: $x_{countevents} \in \mathbb{R}$ a variable representing the number of admission events in the timeline of a patient up to the current admission event (inclusive)

Hence, the feature vector \bar{x}_t is the concatenation of all these variables, encoding the characteristics of both the event and its corresponding patient at one time step of the patient’s trajectory.

B Experiments

B.1 Hyperparameters optimization

B.1.1 RNN model

The set of all possible hyperparameters configuration (i.e. choice of values for hyperparameters) for RNN models is reported in Table 3. These hyperparameters controlled the network architecture design that is represented in Figure 5.

B.1.2 RNNSS model

The hyperparameters configurations for RNNSS model is reported in Table 4, which controlled the network architecture design depicted in Figure 5.

Parameter name	Set / range values	Best / optimal value
Embedding layer (Blue block) dimension	$\{0, \lfloor d/2 \rfloor, \lfloor d/3 \rfloor, \lfloor d/4 \rfloor\}$ where d is input dimension	0
RNN layer (Yellow block)		
RNN type	{LSTM, GRU, Vanilla RNN}	Vanilla RNN
Hidden vector dimension D_h	{8, 16, 32, 64, 128, 256}	16
Number of hidden layers	{1, 2, 3}	1
Dropout probability $p_{dropout}$	{0.15, 0.35, 0.5}	0.35
Embedding layer (Orange block)	$\{0, D_h, \lfloor D_h/2 \rfloor, \lfloor D_h/3 \rfloor, \lfloor D_h/4 \rfloor\}$	0
Non-linear function	{ <i>tanh</i> , <i>ReLU</i> }	<i>ReLU</i>
l_2 -norm regularization λ	$\{10^{-3}, 10^{-2}, 10^{-1}\}$	10^{-2}
Convex combination parameter for the RNN objective function, α	{0.65, 0.8, 0.95}	0.8
Batch size during training $ B $	{8, 16, 32, 64, 128}	64
Optimization algorithm	{Adam}	Adam

Table 3: RNN hyperparameter options (see Figure 5)

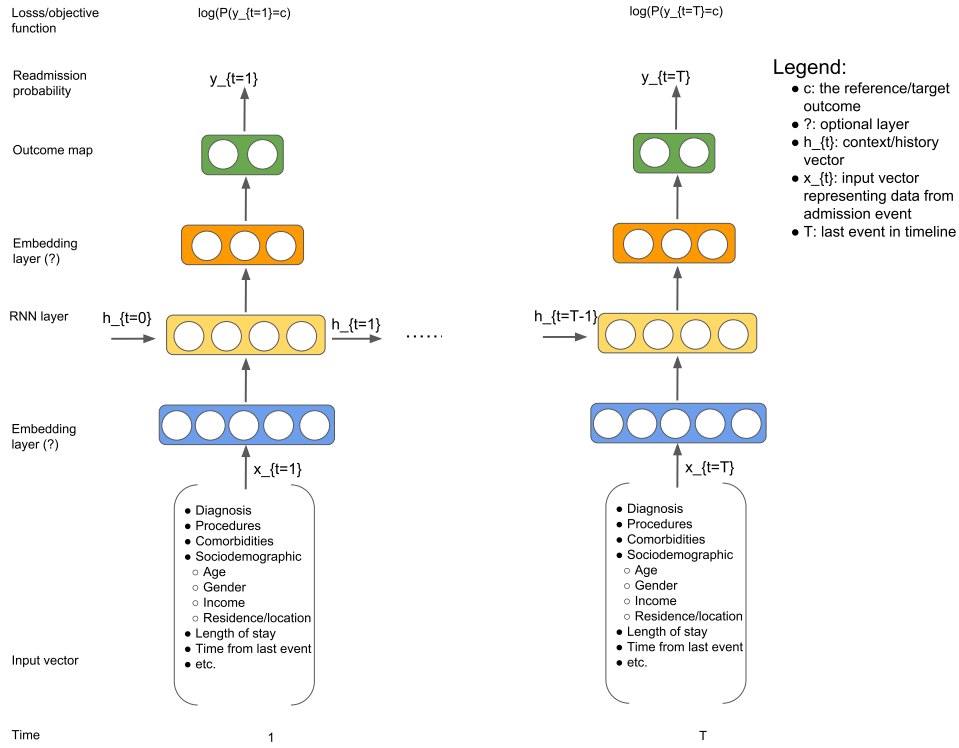


Figure 5: RNN generic model/architecture

Parameter name	Set/range values	Best/optimal value
Embedding layer (Blue block) dimension	$\{0, \lfloor d/2 \rfloor, \lfloor d/3 \rfloor, \lfloor d/4 \rfloor\}$ where d is input dimension	$\lfloor d/2 \rfloor$
RNN layer (Yellow block)		
RNN type	{LSTM, GRU, Vanilla RNN}	GRU
Hidden vector dimension D_h	{8, 16, 32, 64, 128, 256}	128
Number of hidden layers	{1, 2, 3}	1
Dropout probability $p_{dropout}$	{0.15, 0.35, 0.5}	0.15
Embedding layer (Orange block)	$\{0, D_h, \lfloor D_h/2 \rfloor, \lfloor D_h/3 \rfloor, \lfloor D_h/4 \rfloor\}$	$\lfloor D_h/3 \rfloor$
Non-linear function	{ <i>tanh</i> , <i>ReLU</i> }	<i>tanh</i>
l_2 -norm regularization λ	$\{10^{-3}, 10^{-2}, 10^{-1}\}$	10^{-2}
Convex combination parameter for the RNN objective function, α	{0.65, 0.8, 0.95}	0.8
Batch size during training $ B $	{8, 16, 32, 64, 128}	64
Scheduled sampling parameter ρ	{Linear, Exponential, Sigmoid}	Exponential
Optimization algorithm	{Adam}	Adam

Table 4: RNNSS hyperparameter options (see Figure 5)

Parameter name	Set/range values	Best/optimal value
Embedding layer (Blue block) dimension	$\{0, \lfloor d/2 \rfloor, \lfloor d/3 \rfloor, \lfloor d/4 \rfloor\}$ where d is input dimension	$\lfloor d/2 \rfloor$
RNN layer (Yellow block)		
RNN type	{LSTM, GRU, Vanilla RNN}	GRU
Hidden vector dimension D_h	{8, 16, 32, 64, 128, 256}	128
Number of hidden layers	{1, 2, 3}	1
Dropout probability $p_{dropout}$	{0.15, 0.35, 0.5}	0.15
Embedding layer (Orange block)	$\{0, D_h, \lfloor D_h/2 \rfloor, \lfloor D_h/3 \rfloor, \lfloor D_h/4 \rfloor\}$	$\lfloor D_h/3 \rfloor$
Non-linear function	{ <i>tanh</i> , <i>ReLU</i> }	<i>tanh</i>
l_2 -norm regularization λ	$\{10^{-3}, 10^{-2}, 10^{-1}\}$	10^{-2}
Batch size during training $ B $	{8, 16, 32, 64, 128}	64
Optimization algorithm	{Adam}	Adam

Table 5: RNNCRF hyperparameter options (see Figure 6)

Parameter name	Set/range values	Best/optimal value
l_2 -norm regularization λ	$\{10^{-3}, 10^{-2}, 10^{-1}\}$	10^{-2}
Batch size during training $ B $	{8, 16, 32, 64, 128}	64
Optimization algorithm	{Adam}	Adam

Table 6: CRF hyperparameter options (see Figure 7)

B.1.3 RNNCRF model

Similar to RNN models, the set of all possible hyperparameters configuration for models using RNN with CRF is reported in Table 5 along with the network architecture design in Figure 6.

B.1.4 CRF and Neural CRF models

CRF only and Neural CRF models' hyperparameters configuration is reported in Tables 6 and 7 respectively along with the network architecture/design in Figure 7.

B.1.5 CNN model

CNN model's hyperparameters configuration is reported in List 1 along with the network architecture/design in Figure 8.

B.1.6 CNN-Wide model

CNN-Wide model's hyperparameters configuration is reported in List 2 along with the network architecture/design in Figure 9.

Parameter name	Set/range values	Best/optimal value
Embedding layer (Blue block) dimension	$\{0, \lfloor d/2 \rfloor, \lfloor d/3 \rfloor, \lfloor d/4 \rfloor\}$ where d is input dimension	$\lfloor d/2 \rfloor$
Dropout probability $p_{dropout}$	{0.15, 0.35, 0.5}	0.15
Embedding layer (Orange block)	$\{0, \lfloor D_l/2 \rfloor, \lfloor D_l/3 \rfloor, \lfloor D_l/4 \rfloor\}$ where D_l is input dimension from previous layer l	$\lfloor D_l/3 \rfloor$
Non-linear function	{ <i>tanh</i> , <i>ReLU</i> }	<i>tanh</i>
l_2 -norm regularization λ	$\{10^{-3}, 10^{-2}, 10^{-1}\}$	10^{-2}
Batch size during training $ B $	{8, 16, 32, 64, 128}	64
Optimization algorithm	{Adam}	Adam

Table 7: Neural CRF hyperparameter options (see Figure 7)

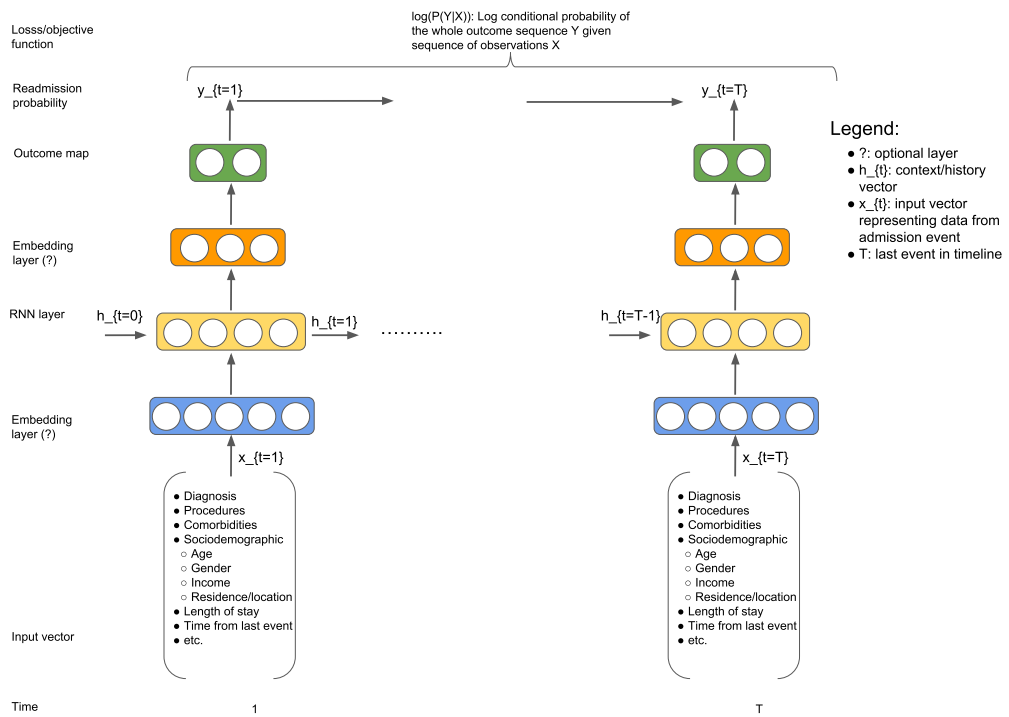


Figure 6: RNNCRF generic model/architecture

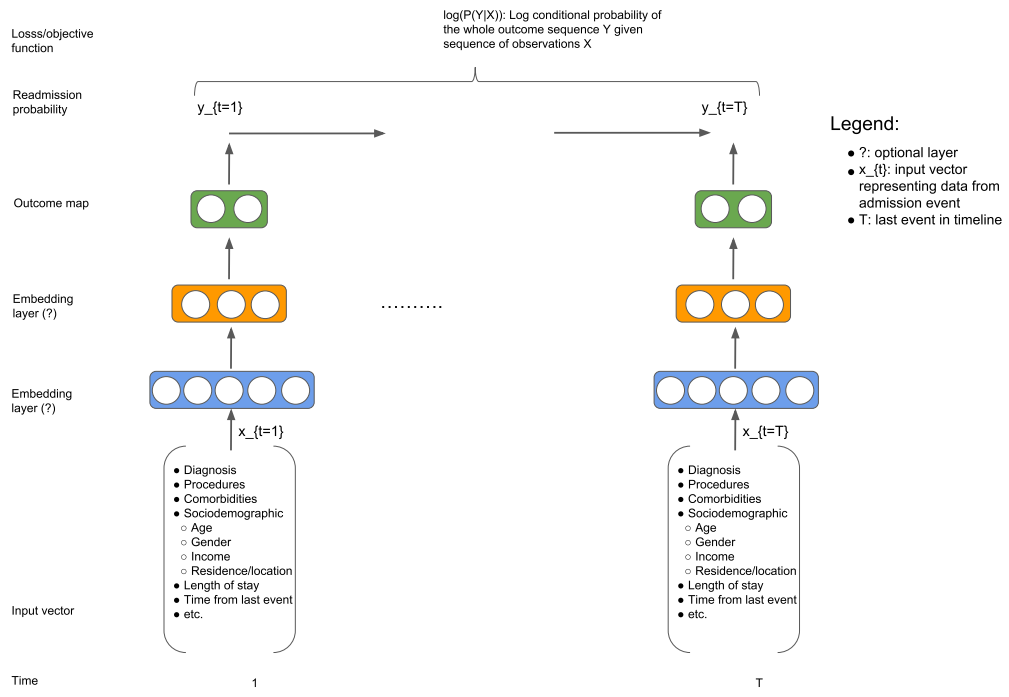


Figure 7: CRF generic model/architecture

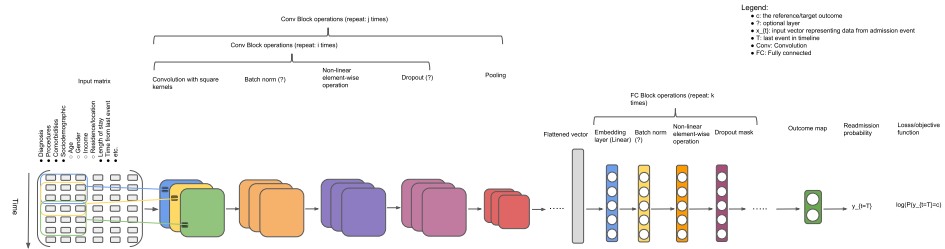


Figure 8: CNN generic model/architecture

List 1 CNN hyperparameter options (see Figure 8). Best parameters are colored in blue.

CNN hyperparameters configuration	
Conv Block operations	
Conv Block J	
Conv Block I	
Square kernel size	$\{3 \times 3, 5 \times 5\}$
Batch norm	$\{True, False\}$
Non-linear function	$\{tanh, ReLU\}$
Dropout	$\{0, 0.15\}$
Starting number of kernels	$\{64, 128, 256\}$
Number of repeats for Conv Block I	$\{1, 2, 3\}$
Pooling	$\{AvgPool, MaxPool\}$
Number of repeats for Conv Block J	$\{7, 8\}$
FC Block operations	
Embedding layer dimension	$\{\lfloor D_l/3 \rfloor, \lfloor D_l/4 \rfloor, \lfloor D_l/5 \rfloor\}$
where D_l is the dimension of flattened feature vector from the last convolutional layer	
Batch norm	$\{True, False\}$
Non-linear function	$\{tanh, ReLU\}$
Dropout	$\{0, 0.15, 0.35, 0.5\}$
Number of repeats for FC Block K	$\{1, 2\}$
l_2 -norm regularization λ	$\{10^{-3}, 10^{-2}, 10^{-1}\}$
Batch size during training $ B $	$\{8, 16, 32\}$
Optimization algorithm	$\{Adam\}$

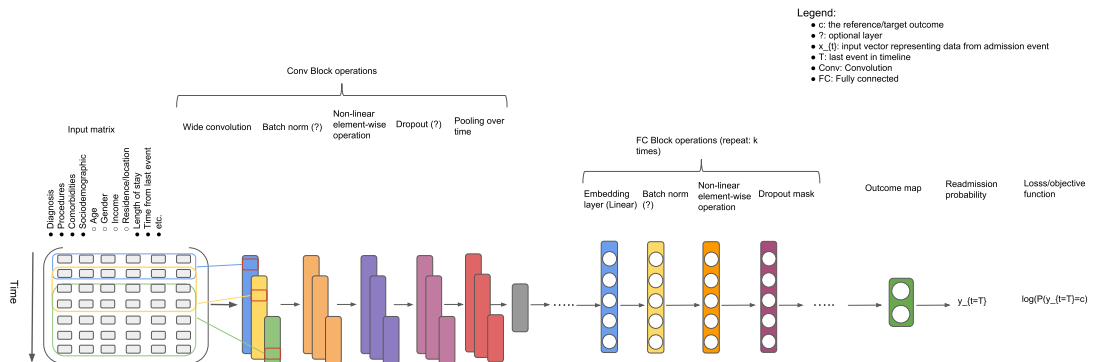


Figure 9: CNN generic model/architecture

List 2 CNNWide hyperparameter options (see Figure 9). Best parameters are colored in blue.

CNN-Wide hyperparameters configuration

- Conv Block operations
 - Rectangular kernel size $\{2 \times d, 3 \times d, 5 \times d\}$ where d is the input dimension
 - Batch norm $\{True, False\}$
 - Non-linear function $\{tanh, ReLU\}$
 - Dropout $\{0, 0.15\}$
 - Number of kernels $\{16, 32, 64, 128\}$
 - Apply padding $\{True, False\}$
 - Pooling $\{AvgPool, MaxPool\}$
 - Number of kernel types used $\{2, 3\}$
- FC Block operations
 - Embedding layer dimension $\{D_l, \lfloor D_l/2 \rfloor, \lfloor D_l/3 \rfloor, \lfloor D_l/4 \rfloor\}$ where D_l is the dimension of flattened feature vector from the last convolutional layer
 - Batch norm $\{True, False\}$
 - Non-linear function $\{tanh, ReLU\}$
 - Dropout $\{0, 0.15, 0.35, 0.5\}$
 - Number of repeats for FC Block K $\{1, 2\}$
- l_2 -norm regularization λ $\{10^{-3}, 10^{-2}, 10^{-1}\}$
- Batch size during training $|B|$ $\{8, 16, 32\}$
- Optimization algorithm $\{Adam\}$

Parameter name	Set/range values	Best/optimal value
l_1 -norm regularization λ	$\{10^{-3}, 10^{-2}, 10^{-1}\}$	10^{-1}
Optimization algorithm	$\{Liblinear, Saga\}$	Liblinear/Saga
Weighting scheme (i.e. weighting training examples)	$\{Balanced, None\}$	Balanced

Table 8: Logistic regression with l_1 -norm regularization (LASSO)

B.1.7 MLP model

MLP model’s hyperparameters configuration is reported in List 3 along with the network architecture/design in Figure 10.

B.1.8 Logistic regression

Logistic regression models’ hyperparameters options are reported in Tables 8 and 9 respectively.

Parameter name	Set/range values	Best/optimal value
l_2/l_1 -norm regularization λ	$\{10^{-3}, 10^{-2}, 10^{-1}, 1\}$	10^{-1}
Optimization algorithm	$\{Liblinear, Saga\}$	Liblinear/Saga
Weighting scheme (i.e. weighting training examples)	$\{Balanced, None\}$	Balanced

Table 9: Logistic regression with l_2 -norm regularization

List 3 NN hyperparameter options (see Figure 10). Best parameters are colored in blue.

NN hyperparameters configuration	
FC Block operations	
Embedding layer dimension	$\{\lfloor D_l/2 \rfloor, \lfloor D_l/3 \rfloor, \lfloor D_l/4 \rfloor\}$
where D_l is the dimension of feature vector from the previous layer	
Batch norm	$\{True, False\}$
Non-linear function	$\{tanh, ReLU\}$
Dropout	$\{0, 0.15, 0.35, 0.5\}$
Number of repeats for FC Block K	$\{1, 2, 3, 4, 5\}$
l_2 -norm regularization λ	$\{10^{-3}, 10^{-2}, 10^{-1}\}$
Batch size during training $ B $	$\{32, 64, 128\}$
Optimization algorithm	$\{Adam\}$

B.2 Feature importance

B.2.1 Logistic regression

The analysis of feature importance is reported in Figure 11, which shows the normalized coefficients of the trained LASSO models averaged across all folds.

B.2.2 RNNCRF model

For the best neural model (RNNCRF), we report the analysis of feature importance according to an approach previously reported in [44]. In short, we iterated over all features attached to the last HF event, and computed the probability of readmission with a feature present or absent. The difference between both probabilities allowed us to quantify a feature’s importance across the five folds (we call this metric *diff_prob* see Fig. 12). Additionally, we computed another variation of the same metric by incorporating the percentage of occurrence of each feature (i.e. when the feature is present) in the computation. In other words, we weighted the computed differences by the percentage of time each feature was present in the dataset (referred to *diff_prob_weighted*, see Fig. 13). A third variation, is computing a ratio (for every feature) dividing the average difference in probability (*diff_prob*) by the average value of the feature when it was present and again weighted by the percentage of occurrence of the feature (*ratio_diff_prob_weighted*, see Fig. 14).

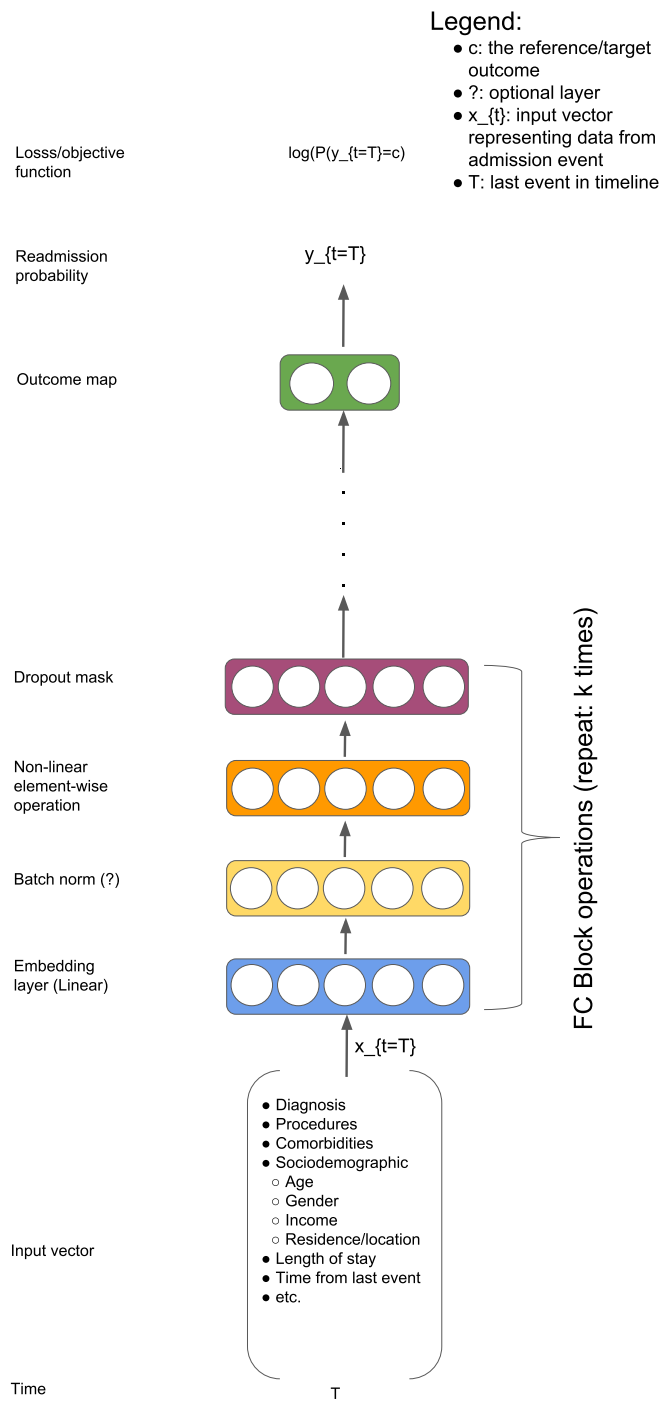


Figure 10: NN generic model/architecture

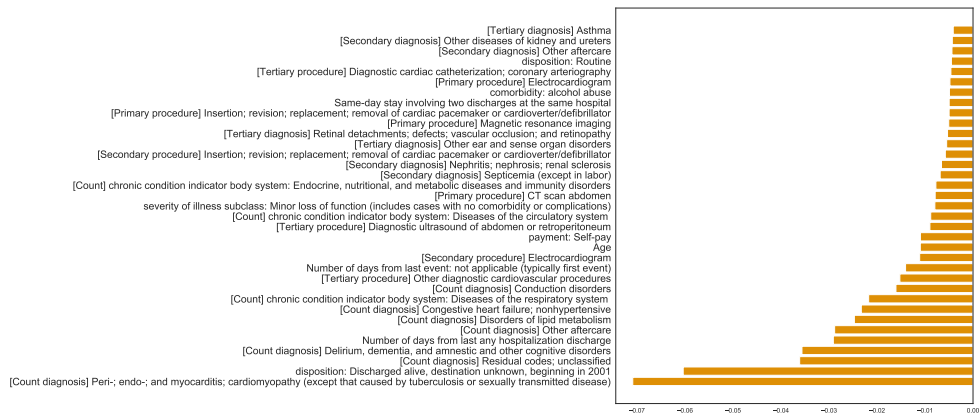
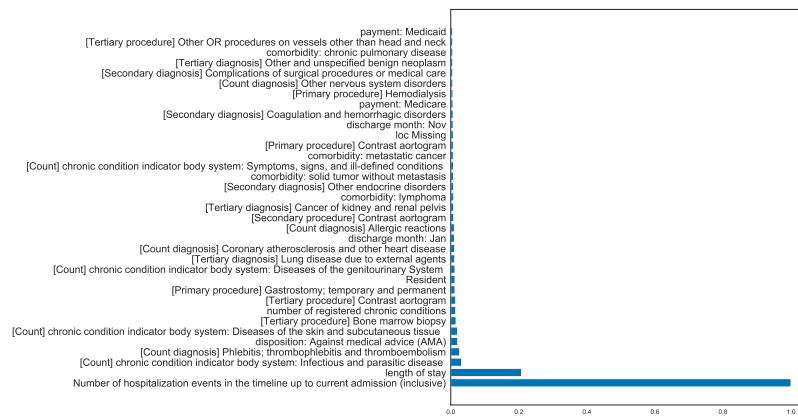


Figure 11: Top-35 features (normalized) in LASSO models contributing to the increase and decrease of log-odds of readmission

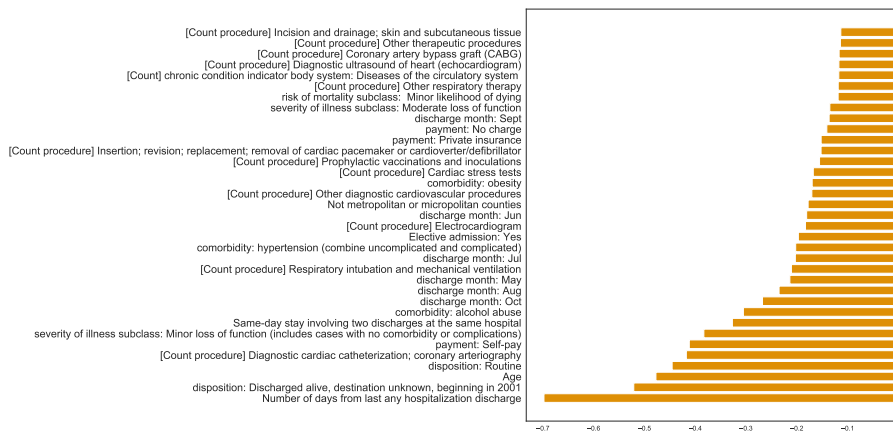
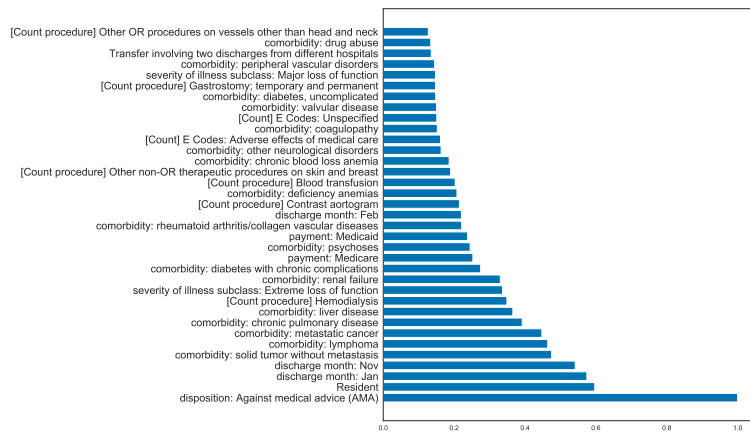


Figure 12: Top-35 features (normalized) in RNNCRF models using *diff_prob* metric

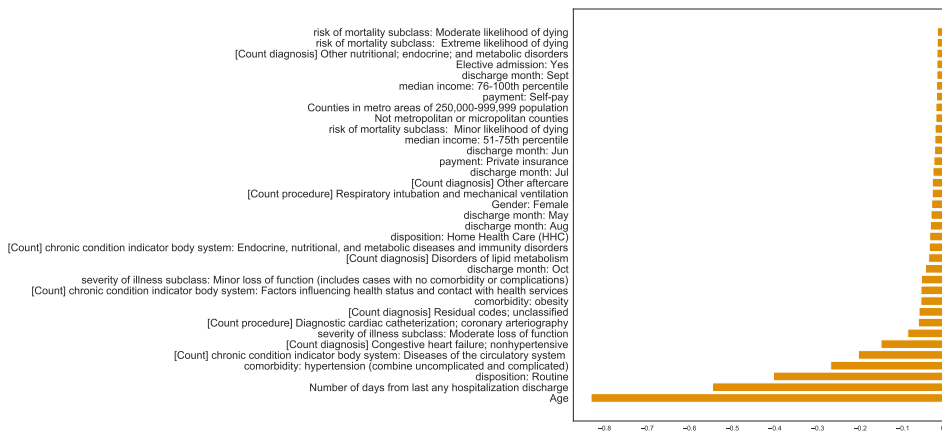
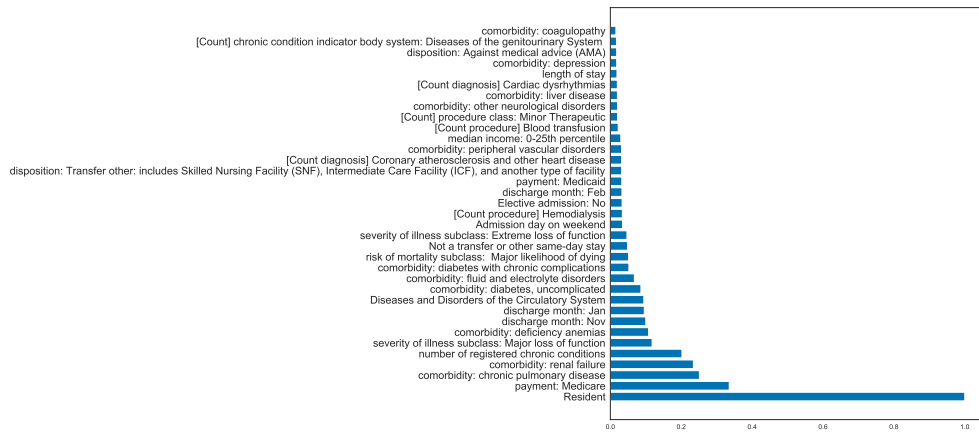


Figure 13: Top-35 features (normalized) in RNNCRF models using *diff_prob_weighted* metric

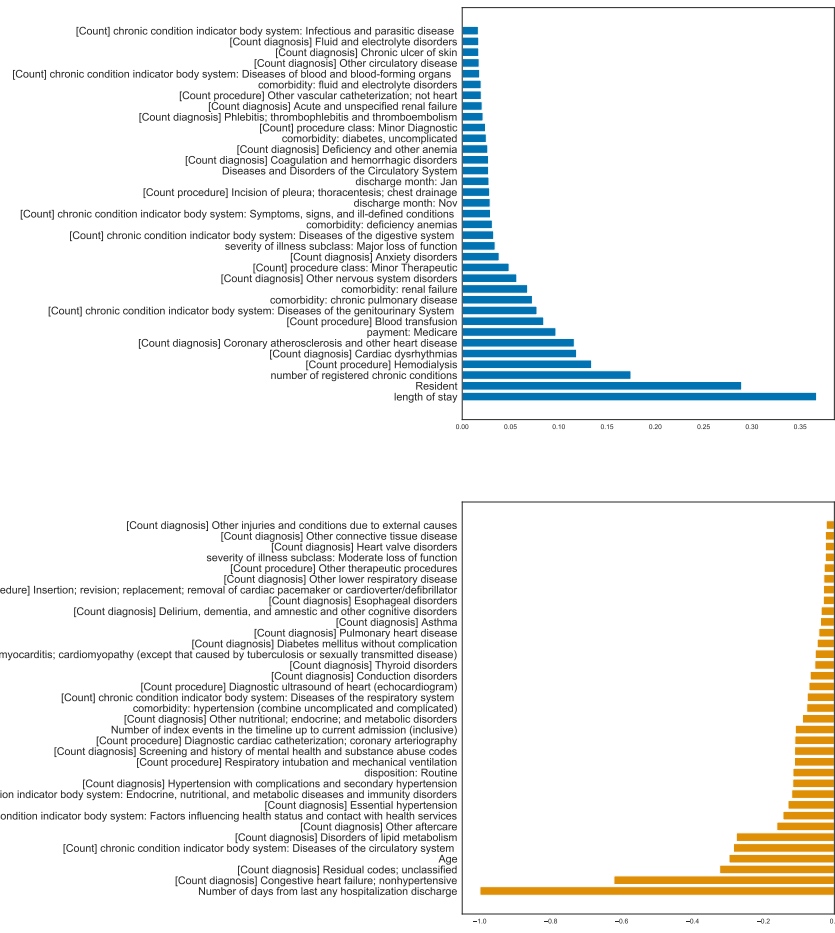


Figure 14: Top-35 features (normalized) in RNNCRF models using *ratio_diff_prob_weighted* metric